Parasite virulence in coinfected hosts: the importance of infection order

Aloïs Dusuel[1*], Luc Bourbon[2*], Emma Groetz[1], Nicolas Pernet[3], Mickaël Rialland[1], Benjamin Roche[4,5], Bruno Faivre[2], Gabriele Sorci[2#]

1. CTM - Center for Translational and Molecular Medicine, INSERM UMR 1231, Université de Bourgogne, 21000 Dijon, France ; LabEx LipSTIC, 21000 Dijon, France

2. Biogéosciences, CNRS UMR 6282, Université de Bourgogne, 6 Boulevard Gabriel, 21000 Dijon, France

3. Plateforme ImaFlow, Université de Bourgogne, Inserm, Institut Agro Dijon, CGFL, CHU Dijon Bourgogne, US58 BioSanD, F-21000 Dijon, France

4. MIVEGEC, IRD, CNRS, Université de Montpellier, 34090 Montpellier, France

5. International Joint Laboratory ELDORADO, IRD/UNAM, Mérida, Yucatán, México

#corresponding author: gabriele.sorci@u-bourgogne.fr

*equal contribution

Abstract

When hosts are simultaneously infected by different pathogens, the severity of the disease might be exacerbated compared to hosts harboring single infections. The reasons underlying these changes in parasite virulence are manifold. Here, we investigated the importance for the infection outcome of order and timing of infection. We used a model of rodent coinfection between two parasites that do not compete for common resources, an intestinal nematode (*Heligmosomoides polygyrus*) and an apicomplexan protozoan (*Plasmodium yoelii*). During single infections, *H. polygyrus* induced only mild disease symptoms. *Plasmodium* produced a substantial reduction in the number of red blood cells but all mice recovered from the infection. A different picture emerged in coinfected hosts. *Heligmosomoides* maintained a profile of mostly asymptomatic infection whatever the order of the infection (first or second). On the contrary, *P. yoelii* incurred substantially higher costs in hosts that had been previously infected with *H. polygyrus* (independently of the timing of infection). We then investigated the possible reasons underlying the increase of *Plasmodium* virulence in coinfected hosts. We found that coinfected hosts were less able to control *Plasmodium* multiplication and to recover from infection-induced anemia. Coinfected hosts had similar levels of erythropoietin and similar renewal of lost red blood cells, resulting in decreased tolerance to *Plasmodium* infection. Experimental administration of erythropoietin in coinfected hosts, partially decreased the severity of disease symptoms and improved tolerance. The detoxification of free heme released during the lysis of red blood cells, and the expression of Th1 and anti-inflammatory cytokine genes were also similar between coinfected and single infected hosts. However, coinfected mice had higher proportions of regulatory T cells expressing the CTLA-4 immune checkpoint, suggesting an enhanced immunosuppressive activity of Tregs. *Plasmodium* infection also induced the exhaustion of $CD8^+$ T cells, as coinfected mice had higher proportions of both PD-1^+ and LAG-3^+ $CD8^+$ T cells, and an increase in the $CD4^+/CD8^+$ ratio. Overall, these results stress the importance of the order of infection as a major determinant of disease severity in coinfected hosts. We discuss the possible epidemiological and evolutionary consequences of these results.

Keywords: coinfection, helminths, *Plasmodium*, nematodes, virulence

Introduction

Coinfection is a widespread phenomenon in plants, wildlife, livestock and humans (Viney and Graham 2013), and describes the occurrence of different parasites/pathogens (hereafter we will use the term parasite as a general term) at the same time in the same individual host. Coinfection has the potential to change the two principal drivers of the infection dynamics, the within host multiplication and the between host transmission (Wait et al. 2021; Imrie et al. 2023), and therefore parasite fitness (Clay and Rudolf 2019) and virulence (i.e., infection-induced damage) (Alizon et al. 2013). During single infections, parasites might have a better access to host resources, while during coinfection, access to resources might be limited if competing parasites share the same infection site or consume the same host resources (Graham 2008; Griffiths et al. 2015). This might affect the within host multiplication rate (for parasites that do multiply within the host) and the transmission rate if coinfection reduces the number of propagules produced per unit of time. This bottom-up regulation of coinfecting parasites might also change the cost paid by the host (e.g., Szabo et al. 2024) if, for instance, the overall host resource consumption exceeds the consumption during single infections. In this case, parasite fitness can also be jeopardized if coinfection compromises the survival of the host. The regulation of the coinfection dynamics might also involve top-down mechanisms, where parasites strive to exploit the host in the face of the immune defenses deployed by the host (Graham 2008). Under this scenario, depending on the nature of the coinfecting parasites, coinfection can have protective [when, for instance, coinfecting parasites elicit similar immune effectors (Filbey et al. 2019)] or antagonistic effects on the host ability to clear the infection (Shen et al. 2019). Specifically, top-down regulation of coinfecting parasites might be compromised when different immune effectors are involved in the process of parasite clearance. Broadly speaking, this is usually the case when hosts are simultaneously infected with microparasites that elicit a Th1 immune response (e.g., viruses and protozoa) and macroparasites that induce a Th2 response (e.g., helminths) (Supali et al. 2010; Ezenwa and Jolles 2011; Ma et al. 2020).

72 Coinfection between micro and macroparasites is a public health issue in several countries of
73 the intertropical areas, given the high prevalence of helminthiases in humans and the overlap with the
74 endemicity of major infectious diseases, such as malaria or AIDS (Webb et al. 2012; Afolabi et al. 2021).
75 Coinfection between gastrointestinal helminths and malaria has attracted attention in the last decades
76 not only to understand if and how helminths might aggravate the severity of malaria symptoms
77 (Degarege et al. 2016; Kwan et al. 2018), but also to forecast the public health effect of deworming
78 campaigns on malaria incidence and severity (Fenton 2013; Budischak et al. 2018), or to assess the
79 potential effect of helminth infection on the efficacy of malaria vaccines (Su et al. 2006; Noland et al.
80 2010; Coelho et al. 2019). However, despite considerable effort, epidemiological studies overall report
81 an inconsistent pattern where coinfection can both result in protection or increased severity of malaria
82 symptoms (Nacher 2011; Salazar-Castañón et al. 2014; Degarege and Erko 2016). This inconsistency
83 can be explained by several factors related, for instance, to the species of coinfecting helminths
84 (Adegnika and Kremsner 2012; Hürlimann et al. 2019). Work conducted using animal models has also
85 reported inconsistent results, depending on mouse strains and parasite species (Segura et al. 2009;
86 Knowles 2011; Kolbaum et al. 2012). Here, we suggest that a previously underestimated factor shaping
87 the outcome of the coinfection might also be the order and timing of the infection with the two
88 parasites (Salazar-Castañón et al. 2018; Karvonen et al. 2019; Billet et al. 2020). In most epidemiological
89 studies, the order of infection is not taken into account because this information is typically not
90 available and might contribute to inflate the heterogeneity of the reported results.

91 The rationale underlying the hypothesis that order of infection is an important driver of the
92 coinfection dynamics rests on the observation that, when coinfecting parasites are regulated through
93 top-down effects, the polarization of the host immune response following the first infection (Hartgers
94 and Yazdanbakhsh 2006; Kotepui et al. 2023) offers a favorable ground for the subsequent infection
95 with the second parasite (Su et al. 2005; Craig and Scott 2017). We explored this question using a
96 model of coinfection with the gastrointestinal nematode *Heligmosomoides polygyrus* (hereafter Hp)
97 and *Plasmodium yoelii* (hereafter Py) in mice. Hp is a model species in immunoparasitology (Reynolds

98 et al. 2012). This nematode is a natural parasite of rodents (Gregory et al. 1992) which elicits a
99 canonical Th2 immune response, orchestrated by Th2 cytokines, such as IL-4, IL-5 and IL-13 (Reynolds
100 et al. 2012). Mice are infected when ingesting infective larvae (L3), and adult worms live in the lumen
101 of the small intestine where they feed on the host's intestinal tissue (Bansemir and Sukhdeo 1994). Py
102 is also a model species for the study of the pathogenesis of malaria and the associated immune
103 response (Olatunde et al. 2022). The strain 17XNL of Py produces self-resolving infections, and
104 although the parasitemia can reach high level, all mice recover from the infection in about four weeks.
105 The cycle in the vertebrate host includes an early hepatic-stage that is followed by the asexual
106 replication within the red blood cells (RBCs) (blood-stage); the lysis of RBCs induces anemia, the typical
107 symptom of malaria infection. Infection with Py stimulates the production of pro-inflammatory
108 cytokines, such as the interferon-gamma (IFN-γ), and therefore polarizes the immune response
109 towards Th1 effectors (Olatunde et al. 2022).

110 Therefore, given that Hp and Py do not share the same ecological niche and do not share
111 common resources for their replication (RBCs for Py), or survival/reproduction (intestinal lumen for
112 Hp), any interference between the two parasites is unlikely to be driven by bottom-up regulation
113 mechanisms. On the contrary, given that the two parasites elicit different immune effectors, and that
114 Th1 and Th2 cytokines have reciprocal inhibitory effects (Paludan 1998), top-down mechanisms are
115 likely candidates to drive the outcome of the coinfection in this system.

116 We conducted a series of experiments with the aim of exploring to what extent the order and
117 timing of the infection with the two parasites drives the infection dynamics and the severity of the
118 disease. We also explored the possible mechanisms underlying the increased disease severity in
119 coinfected hosts. Based on the rationale reported above, we predicted that if the polarization of the
120 immune response towards Th1 (in the case of Py infection) or Th2 (in the case of Hp infection) makes
121 the host more vulnerable to the infection with the other parasite, coinfection should aggravate the
122 symptoms of the disease, compared to single infections.

123

124 **Materials and Methods**
125
126 *Ethical statement*
127
128 Experiments were approved by the Comité d'éthique Grand Campus Dijon of the University of
129 Burgundy and were authorized by the French Ministry of Higher Education and Research under the
130 numbers 33492 and 47573.
131
132 *Experimental animals and infections*
133
134 C57BL/6JRj female mice (7-10 weeks old) were purchased from Janvier Labs (Le Genest-Saint-
135 Isle, France), housed in cages containing 5 individuals under pathogen-free conditions, and maintained
136 under a constant temperature of 24°C and a photoperiod of 12h:12h light:dark with *ad libitum* access
137 to water and standard chow diet (A03-10, Safe, Augny, France). All mice were acclimatized to the
138 housing conditions during, at least, 7 days prior to the start of the experiments, were monitored twice
139 a day to check health status, and euthanized by cervical dislocation under anesthesia with isoflurane
140 either if they reached previously defined end points (and considered as mortality events in the survival
141 analysis) or at specific days post-infection (p.i.) for terminal collection of blood and organs (and
142 considered as censored events in the survival analysis).
143 Mice were infected with *Plasmodium yoelii* 17XNL by intra-peritoneal (i.p.) injection with $5x10^5$
144 infected red blood cells (iRBC) suspended in 0.1 ml of PBS and/or *Heligmosomoides polygyrus bakeri*
145 by oral gavage with L3 larvae (350 larvae suspended in 0.2 ml of drinking water).
146
147 *Experimental groups*
148
149 Mice were randomly assigned to 8 experimental groups (15 to 20 mice per group) as described
150 in figure 1. A control group (group 1) of mice was sham infected (i.p. injection of 0.1 ml of PBS and oral
151 gavage with a 0.2 ml of drinking water). Two groups (groups 2 and 3) received single infections, either
152 with Hp or Py. Five additional groups were coinfected with the two parasites according to specific
153 orders and timings of infection. In one group, mice were simultaneously infected with the two
154 parasites (group 4); in two groups, mice were infected first with Hp and subsequently infected with Py

155 either at day 7 post Hp infection, or at day 28 post Hp infection (groups 5 and 6); in two groups, mice
156 were first infected with Py and subsequently infected with Hp either at day 14 post Py infection, or at
157 day 28 post Py infection (groups 7 and 8). The timings of infection in the coinfection groups correspond
158 to specific stages in the life cycles of the two parasites. Day 7 and 28 post Hp infection correspond to
159 the stage that just precedes the emergence of the adult worms in the intestinal lumen and when the
160 infection has reached a chronic stage, respectively. Day 14 and day 28 post Py infection approximately
161 correspond to the parasitemia peak and the end of the acute phase infection, respectively. The whole
162 experiment was repeated twice, although not all traits were measured in all mice of the two replicates.

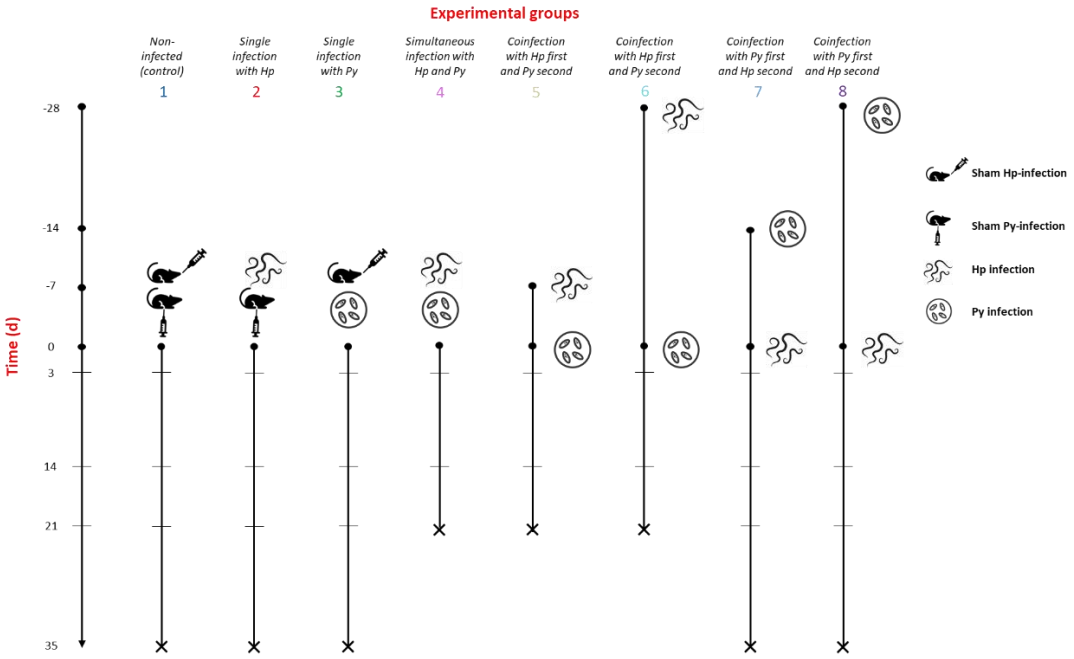

163
164 Figure 1. Schematic view of the experimental setup and groups. Non-infected (group 1) and single (Hp,
165 Py) infected mice (groups 2 and 3) were monitored during 35 days post-infection. One group of
166 coinfected mice (group 4) was simultaneously (the same day) infected with Py and Hp. The other
167 coinfection groups were either infected first with Hp (at day -7 or day -28) and then with Py (groups 5
168 and 6), or infected first with Py (at day -14 or day -28) and then with Hp (groups 7 and 8). Groups 4, 5
169 and 6 were monitored during 21 days post Py infection.
170
171 *Erythropoietin administration*
172
173 Mice (n = 20) were infected with Hp and at day 28 p.i. they were infected with Py. Mice were
174 then split randomly into two groups, one received an i.p. injection of 1 µg of recombinant mouse
175 erythropoietin (rEPO) (959-ME, Bio-Techne, Minneapolis, Minnesota, USA) in 200 µl of PBS at days 0,
176 2 and 4 post Py infection; the other group was injected with 200 µl of PBS only, for control.

177 *Monitoring of health status, hematological and plasma parameters, and Py parasitemia*
178
179 Mice were regularly weighed (at least three times a week) and body mass was used as an
180 integrative marker of host health. Hematological parameters were assessed by collecting 10 µl of blood
181 from the tail tip in 0.5 ml tubes with 1 µl of heparin (Héparine Choay® 25 000 UI/5ml, Sanofi-Aventis,
182 Gentilly, France). These samples were immediately read with a SCIL Vet abc Plus+ hematology analyzer
183 (Horiba Medical, Montpellier, France) to assess RBC concentration and mean globular volume. For
184 mice with Py infection, a drop of blood was smeared on a slide and fixed with methanol. Slides were
185 subsequently stained with a Giemsa RS solution (Carlo Erba Reagents, Val de Reuil, France) (10% v/v in
186 phosphate buffer) for 15 minutes and rinsed with water. Infected RBCs were counted using an optical
187 microscope under magnification x1000, and parasitemia expressed as the proportion of iRBCs.
188 At day 3, 14, 21 and 35 p.i. (post second infection for the coinfection groups), five mice per
189 group were euthanized by cervical dislocation under isoflurane anesthesia, for terminal collection of
190 total peripheral blood and organs. Given the severity of the disease symptoms, the simultaneous
191 infection group and the two coinfection groups first infected with Hp (groups 4, 5, 6) were only
192 monitored up to day 21 post Py infection. Plasma was separated from total blood by centrifugation (7
193 min 3000 rpm 4°C), aliquoted and stored at -80°C.
194 Plasma levels of aspartate aminotransferase (AST) and heme oxygenase-1 (HO-1) were
195 assessed with ab263882 and ab229431 commercial ELISA kits from Abcam (Cambridge, UK),
196 respectively. Plasma levels of mouse erythropoietin (EPO) were assessed with EM28RB commercial
197 ELISA kit from Invitrogen™ (Carlsbad, California, USA). Plates were read with a SpectraMax iD3 multi-
198 mode microplate reader (Molecular Devices, San Jose, California, USA).
199
200 *Organ collection*
201
202 Spleen was removed and weighed. About one third of the spleen was cut and immediately
203 frozen in liquid nitrogen for RT-qPCR, and the remaining was kept on ice in PBS before the flow
204 cytometry staining procedure. A liver slice (left lobe) was also immediately frozen in liquid nitrogen for
205 RT-qPCR.

206 *RNA extraction and qPCR for Hmox-1, IFN-γ, IL-10 and TGF-β1 gene expression*
207
208 Tissues were homogenized in TRIzol™ Reagent (Invitrogen™, Carlsbad, California, USA) under
209 strong agitation using 0.5 mm glass beads and a Precellys® 24 Touch homogenizer (Bertin
210 Technologies, Montigny-le-Bretonneux, France). RNA extraction was performed following the
211 manufacturer's instructions. RNA concentration was measured with a NanoPhotometer® N50 (Implen,
212 Munich, Germany). Reverse transcription was performed with a High-Capacity cDNA Reverse
213 Transcription Kit (Applied Biosystems™, Foster City, California, USA) from 1.5 µg total RNA.
214 Quantitative PCR was performed with PowerUp™ SYBR™ Green Master Mix (Applied Biosystems™) on
215 a QuantStudio™ 3 Real-Time PCR System (Applied Biosystems™). We used two housekeeping genes (β-
216 actin and GAPDH); β-actin provided more consistent values (less intra-group variability) and therefore
217 we used it as the reference gene. Primer sequences are reported in the supplementary material (table
218 S1), and were checked for specificity using the Primer-BLAST tool (NCBI). Melt curve analysis was also
219 performed in all samples to check for the presence of nonspecific amplification products.
220
221 *Spectral flow cytometry*
222
223 Spleens were homogenized with a 70 µm cell strainer and washed two times with PBS to obtain
224 a single-cell suspension. RBCs were removed from suspensions with eBioscience™ RBC Lysis Buffer
225 (Invitrogen™) (3 min incubation at RT). Cells were counted with viability trypan blue dye and
226 dispatched in 96-well V bottom plates to obtain $1x10^7$ live cells/well. Cells were then stained with
227 LIVE/DEAD™ Fixable Blue Dead Cell Stain Kit (Invitrogen™) in PBS for 30 min at 4°C, incubated in stain
228 buffer with BD Fc Block™ (BD Pharmingen™, Franklin Lakes, New Jersey, USA) for 15 min at RT (0.5
229 µg/well), and stained with surface antibodies in brilliant stain buffer (see table S2 for details on the
230 markers used) for 30 min at 4°C. Cells were then fixed and permeabilized with eBioscience™ Foxp3 /
231 Transcription Factor Staining Buffer Set (Invitrogen™) prior intracellular staining in brilliant stain buffer
232 (table S2) for 30 min at RT. Cells were resuspended in stain buffer, filtered with 100 µm nylon mesh
233 and analyzed on a 4-lasers (UV/V/B/R) Aurora™ (Cytek® Biosciences, Fremont, California, USA) spectral

234 flow cytometer in the ImaFlow Facility, part of the US58 BioSanD. Events were gated and analyzed with
235 SpectroFlo® v3.0.0 software (Cytek® Biosciences) (see figures S1 and S2 for the gating strategy).
236
237 *Statistical analyses*
238
239 We used general and generalized linear mixed models (GLMM) to analyze data where each
240 individual mouse was repeatedly sampled, using either a normal distribution or a beta distribution (i.e.,
241 for proportions) of errors. Mouse ID was included in these models as a random intercept. Variables do
242 not necessarily vary linearly with time over the course of the infection. We therefore included squared
243 (and cubic) time p.i. to capture these nonlinear relationships. However, polynomial regression might
244 provide a poor fit to the data. Therefore, we also ran general additive models (GAM) where the degrees
245 of freedom of the smoothing function were chosen based on the generalized cross-validation (GCV)
246 optimization criterion. Some variables had an asymmetrical distribution and were log-transformed to
247 reduce skewness and meet the model assumptions.
248 Differences in survival between groups were analyzed using the Kaplan Meier estimator and
249 significance assessed using a Log-Rank test. For coinfected mice, any mortality that had occurred
250 before the infection with the second parasite was considered as caused by single infections (and
251 therefore included as single infected individuals in the model); any effect of coinfection on survival
252 was, thus, assessed only after the infection with the second parasite. To increase the statistical power,
253 the survival analysis also included additional mice that were followed for a longer period of time (up
254 to day 99 p.i.) for other purposes (i.e., to assess the long-term effect of coinfection on the infection
255 dynamics). Therefore, the survival analysis included up to four replicated datasets.
256 For variables that were measured only once per individual mouse, we ran general or
257 generalized linear models (GLM), depending on the distribution of errors (normal or beta distribution).
258 Post-hoc comparisons between groups were done using LS-means with Bonferroni correction of p
259 values. Differences in sample size across groups reflect missing values, either due to the reaching of
260 the end point or to technical issues during the processing of the sample.

To simplify the interpretation of the results, we ran different sets of models, comparing different groups. First, we compared non-infected mice versus single infections (groups 1, 2 and 3). These models provided us with the baseline information on the intrinsic effect of each parasite when infecting the host alone. Then, we compared single infection versus coinfection groups. This was done separately for Py and Hp by including in the model the corresponding coinfection groups where Py and Hp infected mice that had been previously infected with the other parasite (i.e., groups 3, 4, 5, 6 in one model, and groups 2, 7, 8 in another model). The simultaneous infection group (group 4) was always included in the Py model. Given that the timing of the infection did appear to have minor effects on the response variables, we also ran models where the different coinfection groups were clustered together (groups 4, 5 and 6; groups 7 and 8) and we compared non-infected, single infected and coinfected hosts in the same model. Finally, we ran a model that was restricted to the coinfection groups (excluding the simultaneous infection group) where we could assess the effect of the order of the infection [either Hp first (groups 5 and 6), or Py first (groups 7 and 8)]. All the statistical analyses and figures were done using SAS Studio.

Results

Severity of the disease in single and coinfected hosts

Body mass

We analyzed body mass as percent variation relative to the body mass at the day of the sham-infection for the control group (group 1) and the day of the infection for single and simultaneous infection groups (groups 2, 3 and 4) or the day of the second infection for the coinfection groups (groups 5, 6, 7 and 8). We first compared changes in body mass over time between non-infected and single (Hp, Py) infected mice (groups 1, 2, 3). The model showed that body mass increased linearly over time, at a similar rate for non-infected and single infected mice (table 1, fig. 2a).

290 Table 1. General linear mixed model investigating the changes in body mass (percent variation with
291 respect to day 0) in non-infected and single (Hp and Py) infected mice. We report the parameter
292 estimates with the 95% CI, degrees of freedom (df), F and p values. Mouse ID was included as a random
293 effect to take into account the non-independence of observations for the same individual over time.
294 N = 120 individuals and 774 observations.

Fixed effects		**Estimate**	**95% CI**	**df**	**F**	**p**
Treatment				2,648	0.24	0.7828
	Non-infected	0				
	Hp	-0.47	-3.13/2.20			
	Py	-0.95	-3.60/1.71			
Time		0.54	0.35/0.74	1,648	83.44	<0.0001
Squared time		-0.004	-0.01/0.001	1,648	2.80	0.095
Time*Treatment				2,648	0.12	0.8827
	Non-infected	0				
	Hp	0.007	-0.27/0.29			
	Py	-0.06	-0.33/0.22			
Squared Time*Treatment				2,648	0.88	0.4141
	Non-infected	0				
	Hp	0.0003	-0.01/0.01			
	Py	0.005	-0.003/0.01			
Random effect		**Estimate**	**SE**	**z**	**P**	
ID		16.49	2.49	6.62	<0.0001	

295

296 We then compared changes in body mass in mice that were infected with Py alone and mice
297 that were simultaneously infected or were first infected with Hp and then with Py (groups 4, 5, 6).
298 Although mice in the coinfection groups lost body mass from day 14 post Py infection onwards (table
299 S3, fig. S3a), the squared time by treatment interaction was not statistically significant (table S3). Given
300 that there was no apparent difference in the dynamics of body mass change between the coinfection
301 groups, we ran an additional model where we compared the changes in body mass between non-
302 infected, single Py infected and coinfected groups together (groups 4, 5 and 6). This model showed a
303 strong effect of coinfection on changes in body mass (table 2, fig. 2b), with coinfected mice losing body
304 mass over the course of the infection.

305
306
307
308
309
310
311
312
313

Table 2. General linear mixed model investigating the changes in body mass (percent variation with respect to day 0) in non-infected, single Py infected and coinfected (Hp infecting first and simultaneous infection) mice. We report the parameter estimates with the 95% CI, degrees of freedom (df), F and p values. Mouse ID was included as a random effect to take into account the non-independence of observations for the same individual over time. N = 196 individuals and 1009 observations.

Fixed effects		**Estimate**	**95% CI**	**df**	**F**	**P**
Infection				2,807	3.0	0.0503
	Non-infected	0				
	Single	-4.50	-8.2/-0.8			
	Coinfection	-1.55	-4.6/1.5			
Time		0.60	0.14/1.06	1,807	76.87	<0.0001
Squared time		-0.01	-0.03/0.01	1,807	56.88	<0.0001
Time*Infection				2,807	3.57	0.0285
	Non-infected	0				
	Single	0.88	0.23/1.53			
	Coinfection	0.47	-0.07/1.01			
Squared Time*Infection				2,807	9.72	<0.0001
	Non-infected	0				
	Single	-0.04	-0.07/-0.01			
	Coinfection	-0.05	-0.07/-0.03			
Random effect		**Estimate**	**SE**	**Z**	**p**	
ID		16.7	2.1	7.95	<0.0001	

A different picture emerged when comparing changes in body mass in mice that were infected first with Py and then with Hp. In this case, coinfection (groups 7 and 8) slowed down the rate of body mass gain, but did not produce a loss in body mass (table S4, fig. S3b). As the timing of infection did not have any effect on the changes in body mass, we grouped them and ran an overall model comparing non-infected, single Hp infected and coinfected groups (7 and 8) together. This model confirmed the slight effect of coinfection on the dynamics of body mass change, with coinfected mice having a slower rate of increase in body mass, but not losing mass over time (table 3, fig. 2c). Finally, we ran a model that was only restricted to the four coinfection groups (groups 5, 6, 7 and 8) where mice were either infected first with Hp or with Py. This model confirmed to importance of the order of infection in shaping the dynamics of body mass (table S5, fig. 2d).

Table 3. General linear mixed model investigating the changes in body mass (percent variation with respect to day 0) in non-infected, single Hp infected and coinfected (Py infecting first) mice. We report the parameter estimates with the 95% CI, degreed of freedom (df), F and p values. Mouse ID was included as a random effect to take into account the non-independence of observations for the same individual over time. N = 155 individuals and 869 observations.

Fixed effects		**Estimate**	**95% CI**	**df**	**F**	**p**
Infection				2,708	1.06	0.3477
	Non-infected	0				
	Single	-0.52	-2.61/1.57			
	Coinfection	0.8	-1.042.64			
Time		0.54	0.40/0.68	1,708	86.46	<0.0001
Squared time		-0.004	-0.008/-0.0005	1,708	0.58	0.4468
Time*Infection				2,708	22.19	<0.0001
	Non-infected	0				
	Single	0.007	-0.2/0.21			
	Coinfection	-0.52	-0.70/-0.34			
Squared Time*Infection				2,708	9.50	<0.0001
	Non-infected	0				
	Single	0.0007	-0.005/0.006			
	Coinfection	0.01	0.005/0.015			
Random effect		**Estimate**	**SE**	**z**	**P**	
ID		11.96	1.62	7.37	<0.0001	

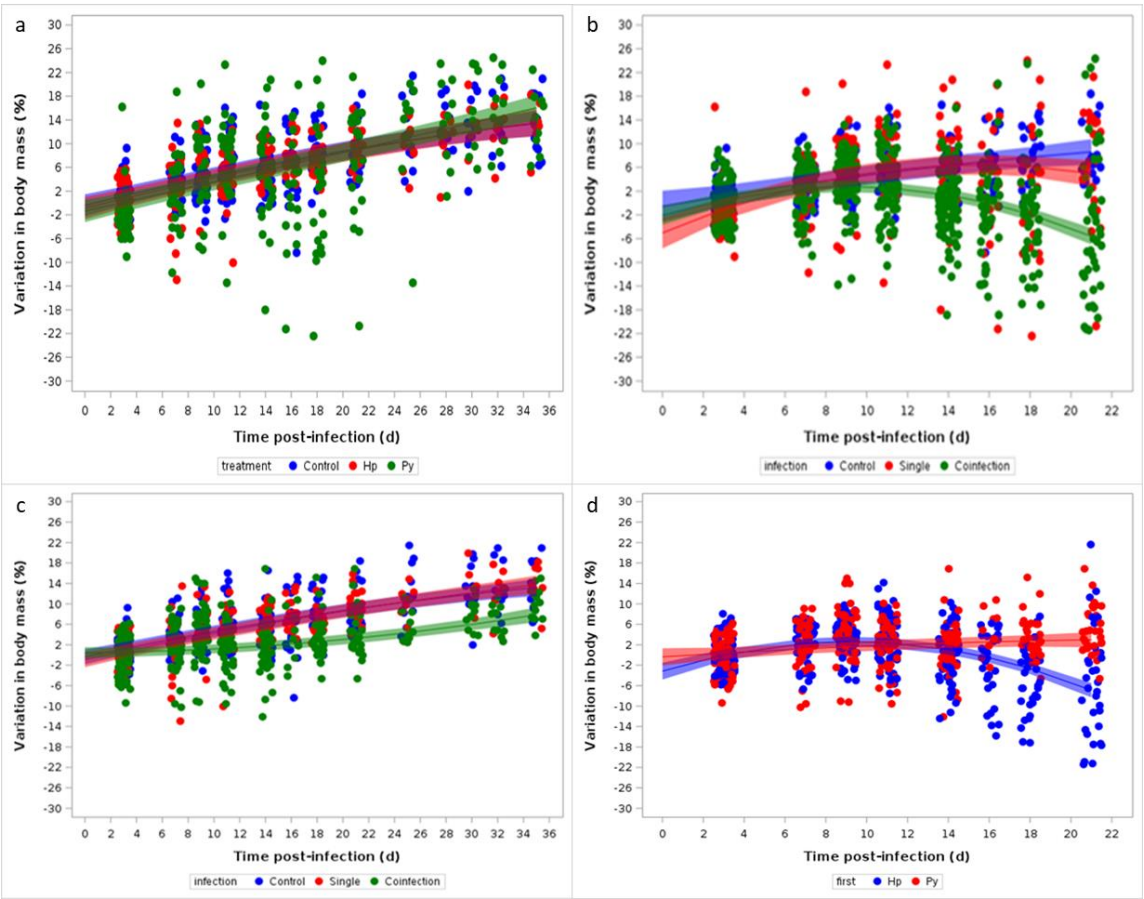

342 Figure 2. Changes in body mass over the course of the infection. Body mass is expressed as percent
343 variation with respect to body mass at day 0 [for the non-infected, single (Hp, Py) infected, and
344 simultaneous infection groups] or at the day of the second infection for the sequential coinfection
345 groups. a) Changes in body mass for non-infected and single (Hp, Py) infected mice; b) Changes in body
346 mass for non-infected, single Py infected and coinfected (Hp infecting first and simultaneous infection)
347 groups; c) Changes in body mass for non-infected, single Hp infected and coinfected (Py infecting first)
348 groups; d) Changes in body mass for coinfected groups depending on the order of the infection (Hp
349 infecting first or Py infecting first). Dots represent the raw data, the lines represent the fit of a GLMM,
350 and the shaded area around the line the 95% CI.
351

352 Therefore, coinfection aggravated one of the most integrative symptoms of disease severity,
353 but the magnitude of the aggravating effect was strongly dependent on the order of the infection.

354
355 *Splenomegaly*
356
357 Splenomegaly (i.e., the enlargement of the spleen) is another prominent symptom of the
358 infection with Hp or Py. We measured spleen mass at day 3, 14, 21 and 35 p.i. and confirmed that
359 single infection induced splenomegaly of different magnitude depending on the parasite (table S6, fig.
360 3a). When comparing groups infected first with Hp and then with Py (plus the simultaneous infection,
361 groups 4, 5, 6), coinfection only had a mild initial effect on splenomegaly at day 3 post Py infection
362 compared to single Py infected hosts (Table S7), but by day 14 p.i. the differences vanished (fig. S4a).
363 This result was corroborated when comparing non-infected, single Py infected and coinfected groups
364 together (Table S8, fig. 3b).
365 When comparing the effect of coinfection in groups that were first infected by Py (groups 7
366 and 8), we found only a moderate increase in spleen mass, essentially as a consequence of the residual
367 enlargement due to the previous Py infection, since the difference between single Hp infection and
368 coinfection groups tended to vanish over time (table S9 and table S10, fig. 3c).
369 The asymmetric effect of infection order on splenomegaly was best captured by the model on
370 the four coinfection groups (groups 5, 6, 7 and 8) where mice were either infected first with Hp or with
371 Py. This model showed that spleen mass increased over the course of the infection only when mice
372 were first infected with Hp and subsequently by Py (table S11, fig. 3d).

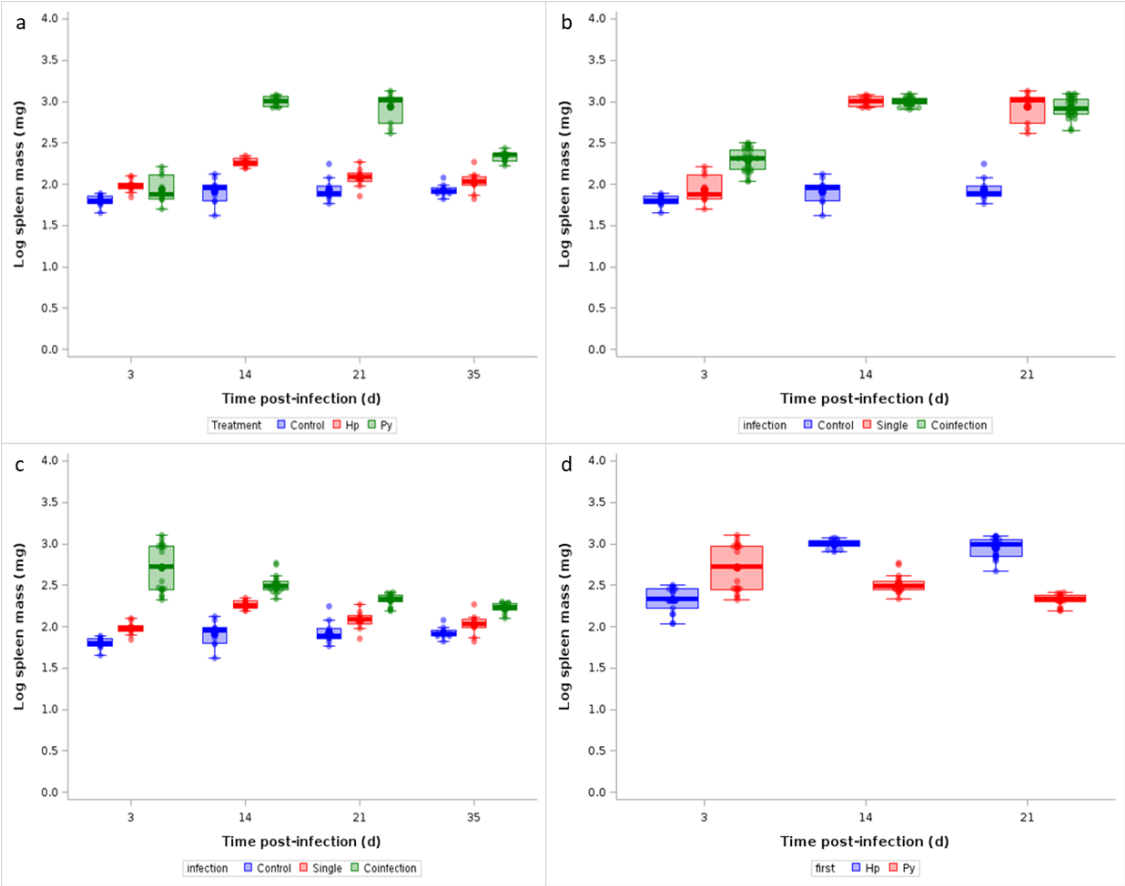

Figure 3. Changes in log_{10} transformed spleen mass (mg) over the course of the infection. a) Changes in spleen mass for non-infected and single (Hp, Py) infected mice; b) Changes in spleen mass for non-infected, single Py infected and coinfected (Hp infecting first and simultaneous infection) groups; c) Changes in spleen mass for non-infected, single Hp infected and coinfected (Py infecting first) groups; d) Changes in spleen mass for coinfected groups depending on the order of the infection (Hp infecting first or Py infecting first). Dots represent the raw data, the boxes represent the interquartile range (IQR), the horizontal lines the median, and whiskers the range of data within 1.5 the IQR.

Therefore, as for body mass, coinfection affected splenomegaly in an asymmetric way, depending on infection order.

Marker of liver damage

We compared a marker of liver damage (aspartate aminotransferase, AST) in plasma at day 21 p.i. in non-infected and single (Hp, Py) infected mice, and found that Py infected mice had moderately higher levels of AST compared to non-infected hosts (GLM, $F_{2,23} = 4.45$, $p = 0.0218$, n = 26 individuals; fig. 4a). Coinfection did aggravate liver damage in the groups where Py followed the Hp infection (plus simultaneous infection, groups 4, 5, 6) (GLM, $F_{3,36} = 4.28$, $p = 0.0111$, n = 40; fig. S5a), and this effect

392 was confirmed when analyzing non-infected, single Py infected and coinfected mice together in the
393 same model (GLM, $F_{2,45} = 4.22$, $p = 0.0209$, $n = 48$; fig. 4b).
394 We found rather similar effects of coinfection when analyzing the groups where Hp follows Py
395 (groups 7 and 8), with coinfection groups having higher AST levels compared to non-infected and single
396 Hp infected groups (GLM, $F_{2,29} = 4.96$, $p = 0.0141$, $n = 32$; fig. 4c, fig. S5b). As a consequence, there was
397 no effect of infection order in the coinfection groups (groups 5, 6, 7 and 8) on AST level at day 21 p.i.
398 (GLM, $F_{1,35} = 0.28$, $p = 0.5976$, $n = 37$; fig. 4d).

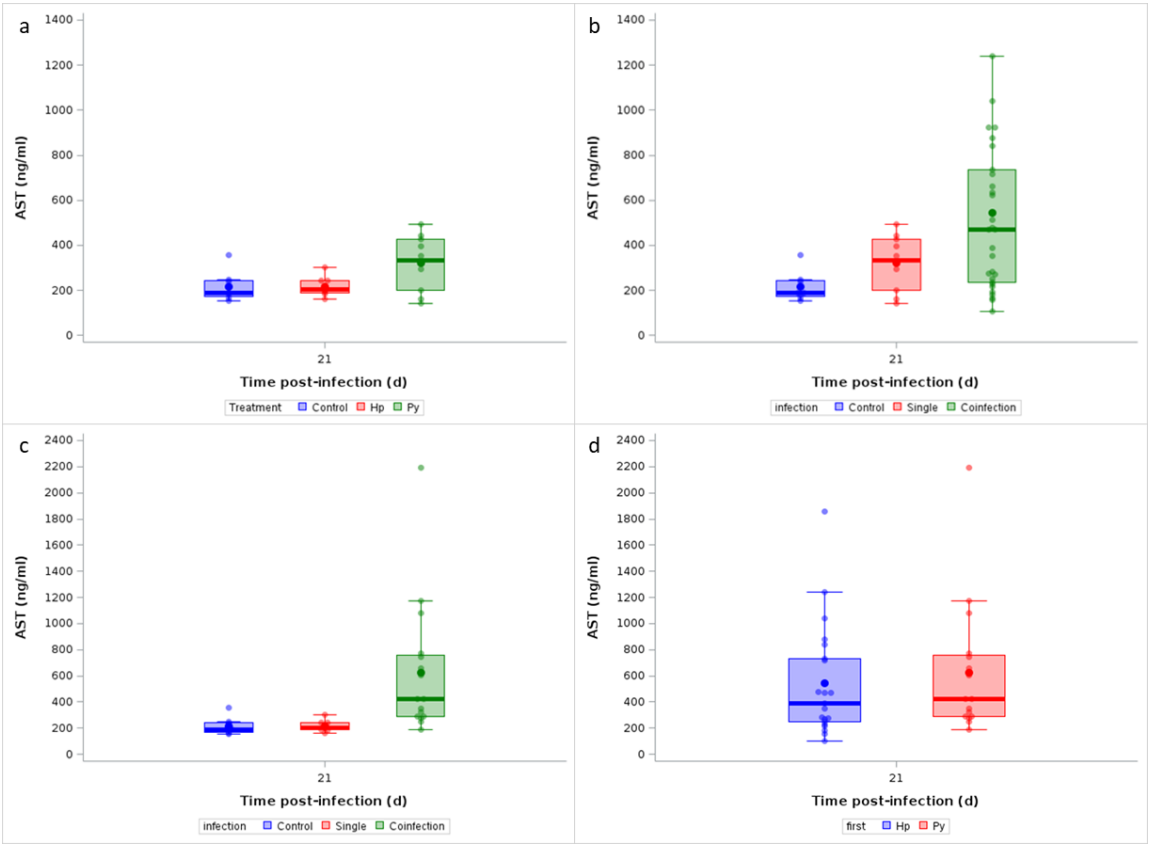

399
400 Figure 4. Effect of infection and coinfection on liver damage. a) Levels of aspartate aminotransferase
401 (AST, ng/ml) in the plasma at day 21 p.i. in non-infected and single (Hp, Py) infected mice; b) AST level
402 in plasma of non-infected, single Py infected and coinfected (Hp infecting first and simultaneous
403 infection) groups at day 21 p.i.; c) AST level in plasma of non-infected, single Hp infected and coinfected
404 (Py infecting first) groups at day 21 p.i.; d) AST level in plasma of coinfected mice, depending on the
405 order of the infection (Hp infecting first or Py infecting first) at day 21 post-infection. Dots represent
406 the raw data, the boxes represent the interquartile range (IQR), the horizontal lines the median, and
407 whiskers the range of data within 1.5 the IQR.
408
409 *Survival*
410
411 In agreement with the pattern of change in body mass over the course of the infection, we did
412 not find any difference in the survival rate between non-infected and single infected mice (Log-Rank

413 test $\chi^2_2 = 0.92$, $p = 0.6315$, $n = 229$; fig. 5a). Timing of infection did not affect host survival in coinfected
414 groups when Py followed the Hp infection (plus simultaneous infection, groups 4, 5 and 6) (Log-Rank
415 test $\chi^2_2 = 1.45$, $p = 0.4844$, $n = 148$; fig. S6), we therefore compared the coinfection groups together
416 with the non-infected and single Py infection and found a strong effect of coinfection (Log-Rank test
417 $\chi^2_2 = 26.02$, $p < 0.0001$, $n = 282$; fig. 5b).

418 There was no host mortality in the coinfection groups where Hp followed Py (groups 7 and 8),
419 whatever the timing of the infection. Therefore, there was no difference in the mortality rate of non-
420 infected, single Hp infected and coinfected groups (groups 7 and 8) (Log-Rank test $\chi^2_2 = 2.34$, $p =$
421 0.3099, $n = 229$; fig. 5c). As a consequence, order of infection was a strong predictor of host mortality
422 in the coinfection groups (groups 5, 6, 7 and 8) (Log-Rank test $\chi^2_1 = 13.47$, $p = 0.0002$, $n = 189$; fig. 5d).

423 Overall, these results show that order of infection has a paramount effect on the severity of
424 the symptoms and therefore on parasite virulence (infection-induced damage), with Hp infection
425 producing mild symptoms whatever the order of the infection, and Py becoming substantially more
426 virulent when infecting hosts already harboring the nematode. However, the timing of infection had
427 virtually no effect on disease severity.

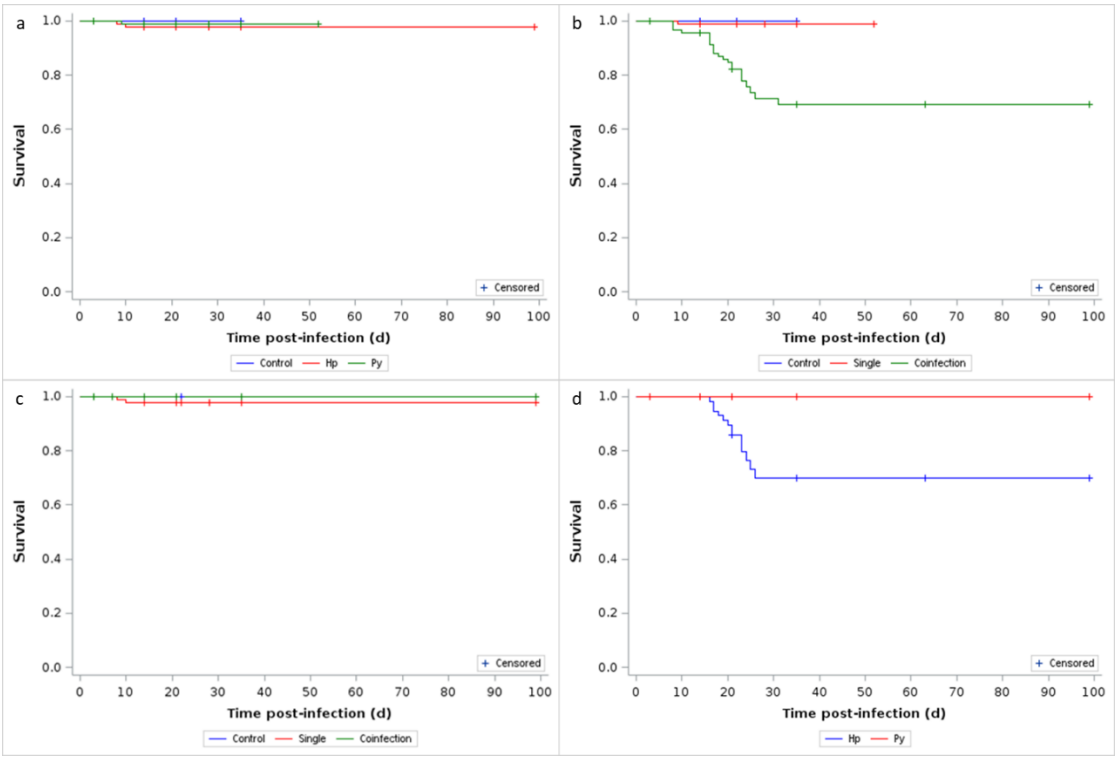

428

429 Figure 5. Effect of infection and coinfection on host survival. a) Survival curves for non-infected and
430 single (Hp, Py) infected mice; b) Survival curves for non-infected, single Py infected and coinfected (Hp
431 infecting first and simultaneous infection) mice; c) Survival curves for non-infected, single Hp infected
432 and coinfected (Py infecting first) mice; d) Survival curves for coinfected mice depending on the order
433 of infection (Hp infecting first or Py infecting first). Crosses indicate censored observations.
434
435 ***Py parasitemia***
436
437 If previous infection with Hp makes the ground more favorable for a subsequent Py infection,
438 we should expect higher parasitemia in coinfected hosts (groups 4, 5, 6) compared to single Py
439 infection. During single infection, parasitemia reached a peak at around day 16 p.i., and then the
440 infection resolved by day 30 (fig. 6a; fig. S7). Given that the coinfection groups (groups 4, 5 and 6) were
441 stopped at day 21 p.i., we could only compare the rising and the early declining stages of the
442 parasitemia. The model showed that coinfected groups reached higher parasitemia and that, contrary
443 to the single infection group, the parasitemia of coinfected mice kept increasing up to day 21 p.i. (table
444 S12 and table 4, fig. S8 and fig. 6b).
445
446 Table 4. General linear mixed model investigating the changes in parasitemia (proportion of iRBC) in
447 single Py infection and coinfected (Hp infecting first and simultaneous infection). We report the
448 parameter estimates with the 95% CI, degrees of freedom (df), F and p values. Mouse ID was included
449 as a random effect to take into account the non-independence of observations for the same individual
450 over time. The distribution of errors was modelled using a beta distribution. N = 151 individuals and
451 665 observations.

Fixed effects		**Estimate**	**95% CI**	**df**	**F**	**p**
Infection				1,510	11.3	0.0008
	Single	0				
	Coinfection	1.95	0.81/3.1			
Time		1.05	0.9/1.2	1,510	428.25	<0.0001
Squared time		-0.03	-0.04/0.02	1,510	230.38	<0.0001
Time*Infection				1,510	12.12	0.0005
	Single	0				
	Coinfection	-0.3	-0.48/-0.13			
Squared Time*Infection				1,510	17.63	<0.0001
	Single	0				
	Coinfection	0.01	0.007/0.019			
Random effect		**Estimate**	**SE**	**z**	**p**	
ID		0.139	0.032	4.32	<0.0001	

452
453

454 Therefore, as expected, previous infection with Hp made a more favorable ground for
455 subsequent Py infection that replicated more and for longer time in coinfected mice. Enhanced
456 persistent parasitemia might thus explain the observed increase of Py virulence in coinfected hosts
457 through specific costs incurred during the asexual reproduction of Py.

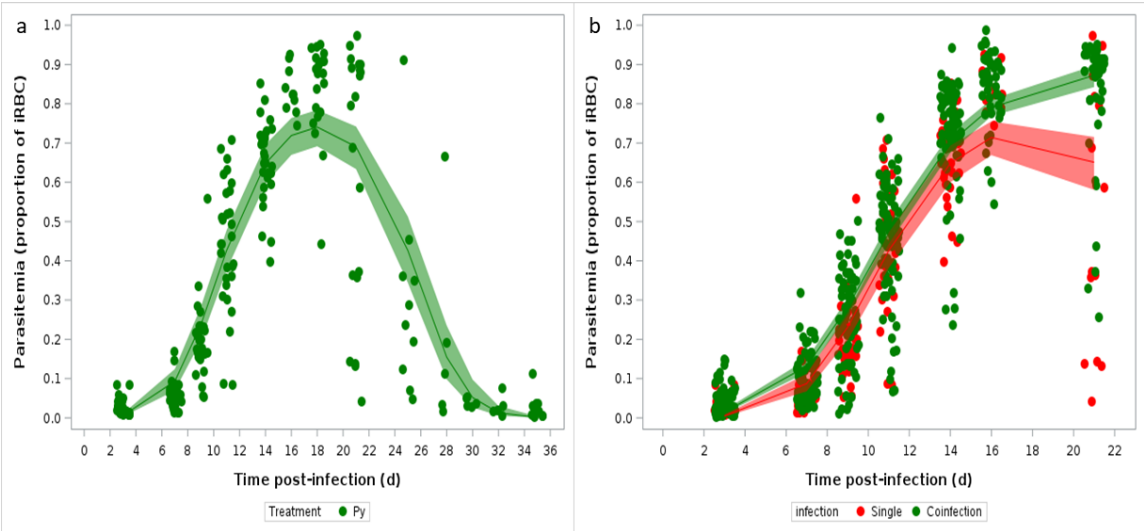

458
459 Figure 6. Changes in parasitemia over the course of the infection. a) Changes in Py parasitemia
460 (proportion of iRBCs counted using optical microscopy) in single infected mice over time; b) Changes
461 in Py parasitemia (proportion of iRBCs) in single infected and coinfected (Hp infecting first and
462 simultaneous infection) mice. Dots represent the raw data, the lines represent the fit of the GLMM,
463 and the shaded area around the line the 95% CI.
464
465 ***Specific costs of Py infection***
466
467 The principal cost induced by Py infection is related to the anemia caused by the lysis of RBCs
468 during the asexual reproduction of the parasite (Olatunde et al. 2022). We therefore assessed the
469 changes in RBC counts over the course of the infection. First, we compared changes in RBC counts
470 between non-infected and single (Hp, Py) infections. As expected, Py infection produced a sharp
471 decline in the number of RBCs, while there was no difference between non-infected and Hp single
472 infection (table 5, fig. 7a, fig. S9), corroborating the idea that Py and Hp do not compete for common
473 resources.
474
475
476

477 Table 5. General linear mixed model investigating the changes in RBC counts (10^6/µl) in non-infected
478 and single (Hp, Py) infected mice. We report the parameter estimates with the 95% CI, degrees of
479 freedom (df), F and p values. Mouse ID was included as a random effect to take into account the non-
480 independence of observations for the same individual over time. N = 60 individuals and 360
481 observations.

Fixed effects		**Estimate**	**95% CI**	**df**	**F**	**p**
Treatment				2,291	5.27	0.0056
	Non-infected	0				
	Hp	0.709	0.101/1.361			
	Py	0.967	0.36/1.574			
Time		-0.224	-0.35/-0.098	1,291	197.56	<0.0001
Squared time		0.013	0.003/0.023	1,291	86.17	<0.0001
Cubic time		-0.0002	-0.0004/-5^{e-6}	1,291	39.83	<0.0001
Time*Treatment				2,291	36.27	<0.0001
	Non-infected	0				
	Hp	-0.163	-0.344/0.017			
	Py	-0.735	-0.913/-0.557			
Squared time*Treatment				2,291	9.55	<0.0001
	Non-infected	0				
	Hp	0.011	-0.003/0.025			
	Py	0.031	0.017/0.045			
Cubic time*Treatment				2,291	2.22	0.1101
	Non-infected	0				
	Hp	-0.0002	-0.0005/0.00008			
	Py	-0.0003	-0.0006/-0.00001			
Random effect		**Estimate**	**SE**	**z**	**P**	
ID		0.1415	0.061	2.37	0.0089	

482

483 Coinfected groups (groups 4, 5, 6) had a similar drop in the count of RBCs (table S13, fig. S10),
484 and we clustered them and compared the changes in RBC counts between non-infected, single Py
485 infected and coinfected mice (groups 4, 5, 6). The model showed that coinfected mice still had low
486 levels of RBCs at day 21 p.i. compared to single Py infected mice that had already started the recovery
487 phase (table 6, fig. 7b, fig. S10c).

488

489

490

491

492

493 Table 6. General linear mixed model investigating the changes in RBC count (10^6/µl) in non-infected,
494 single Py infected and coinfected (Hp infecting first and simultaneous infection) mice. We report the
495 parameter estimates with the 95% CI, degreed of freedom (df), F and p values. Mouse ID was included
496 as a random effect to take into account the non-independence of observations for the same individual
497 over time. N = 94 individuals and 476 observations.

Fixed effects		**Estimate**	**95% CI**	**df**	**F**	**p**
Infection				2,373	1.70	0.1840
	Non-infected	0				
	Single	0.263	-0.40/0.92			
	Coinfected	-0.24	-0.79/0.31			
Time		-0.074	-0.29/0.14	1,373	0.03	0.8556
Squared time		-0.006	-0.032/0.021	1,373	67.42	<0.0001
Cubic time		0.0004	-0.0004/0.001	1,373	108.37	<0.0001
Time*Infection				2,373	0.73	0.4826
	Non-infected	0				
	Single	0.166	-0.14/0.471			
	Coinfected	0.024	-0.23/0.28			
Squared Time*Infection				2,373	11.62	<0.0001
	Non-infected	0				
	Single	-0.09	-0.127/-0.052			
	Coinfected	-0.057	-0.088/-0.026			
Cubic Time*Infection				2,373	17.96	<0.0001
	Non-infected	0				
	Single	0.004	0.002/0.005			
	Coinfected	0.002	0.001/0.003			
Random effect		**Estimate**	**SE**	**z**	**P**	
ID		0.37	0.084	4.37	<0.0001	

498

499 Infection-induced anemia stimulates erythropoiesis with the aim of restoring homeostatic RBC
500 counts. We therefore investigated whether coinfection impaired the host capacity to repair the
501 damage (here the loss of RBCs) caused by the infection. To this purpose, we assessed the production
502 of erythropoietin (EPO) (at day 14 and 21 p.i.) and the mean globular volume (MGV) that reflects the
503 proportion of reticulocytes among the total RBCs.

504 Mice with single Py infection produced EPO in response to the loss of RBCs compared to non-
505 infected individuals (GLM, $F_{1,34}$ = 113.53, p < 0.0001, n = 38; fig. 7c). However, despite having lower
506 RBC counts, coinfected hosts (groups 4, 5, 6) did not produce more EPO compared to single Py infected
507 mice, neither when including each coinfection group separately in the model (GLM, $F_{3,67}$ = 2.24, p =
508 0.0917, n = 75; fig. S11), nor when grouping them (post hoc comparison of LS-means between single
509 infection and coinfection with Bonferroni correction, p = 0.3096, n = 94; fig. 7c)

510 This result was mirrored by the change of MGV over the course of the infection. Py infected
511 mice had a sharp increase in the MGV between day 11 and 21 p.i., compared to non-infected and Hp
512 infected mice, indicating a higher proportion of reticulocytes among RBCs (table 7, fig. 7d, fig. S12).
513 However, changes in MGV were similar between single Py infection and the coinfection groups (groups
514 4, 5, 6) (table 8, fig. 7e, table S14, fig. S13).

515

516 Table 7. General linear mixed model investigating the changes in mean globular volume (fL) in non-
517 infected and single (Hp, Py) infected mice. We report the parameter estimates with the 95% CI, degrees
518 of freedom (df), F and p values. Mouse ID was included as a random effect to take into account the
519 non-independence of observations for the same individual over time. N = 60 individuals and 360
520 observations.

Fixed effects		**Estimate**	**95% CI**	**df**	**F**	**p**
Treatment				2,291	1.90	0.151
	Non-infected	0				
	Hp	0.658	-2.108/3.424			
	Py	-1.975	-4.738/0.789			
Time		0.486	-0.09/1.061	1,291	8.14	0.0046
Squared time		-0.026	-0.071/0.02	1,291	0.94	0.3326
Cubic time		0.0003	-0.0006/0.001	1,291	8.0	0.005
Time*Treatment				2,291	3.20	0.0423
	Non-infected	0				
	Hp	-0.529	-1.354/0.295			
	Py	0.53	-0.284/1.343			
Squared Time*Treatment				2,291	3.37	0.0358
	Non-infected	0				
	Hp	0.032	-0.033/0.097			
	Py	0.084	0.02/0.148			
Cubic Time*Treatment				2,291	10.55	<0.0001
	Non-infected					
	Hp	-0.0005	-0.002/0.0008			
	Py	-0.003	-0.004/-0.002			
Random effect		**Estimate**	**SE**	**z**	**P**	
ID		2.86	1.18	2.42	0.0078	

521

522

523

524

525

526

527 Table 8. General linear mixed model investigating the changes in mean globular volume (fL) in non-
528 infected, single Py infected and coinfected (Hp infecting first and simultaneous infection) mice. We
529 report the parameter estimates with the 95% CI, degrees of freedom (df), F and p values. Mouse ID
530 was included as a random effect to take into account the non-independence of observations for the
531 same individual over time. N = 94 individuals and 476 observations.

Fixed effects		**Estimate**	**95% CI**	**df**	**F**	**P**
Infection				2,373	1.05	0.3518
	Non-infected	0				
	Single	2.1	-1.05/5.25			
	Coinfection	1.7	-0.91/4.31			
Time		0.6	-0.54/1.75	1,373	45.87	<0.0001
Squared time		-0.04	-0.18/0.1	1,373	111.07	<0.0001
Cubic time		0.0008	-0.004/0.005		109.01	
Time*Infection				2,373	17.09	<0.0001
	Non-infected	0				
	Single	-4.36	-5.98/-2.73			
	Coinfection	-3.56	-4.92/-2.21			
Squared Time*Infection				2,373	30.02	<0.0001
	Non-infected	0				
	Single	0.71	0.51/0.90			
	Coinfection	0.58	0.41/0.74			
Cubic Time*Infection				2,373	27.42	<0.0001
	Non-infected	0				
	Single	-0.02	-0.03/0.016			
	Coinfection	-0.02	-0.02/0.012			
Random effect		**Estimate**	**SE**	**z**	**p**	
ID		4.28	1.25	3.44	0.0003	

532

533 Given that coinfected hosts harbored more parasites than single infected hosts, a similar rate
534 of renewal of lost RBCs should result in a reduction in tolerance in coinfected mice. We defined
535 tolerance as the slope of the regression of RBC counts on parasitemia, the steeper the slope the weaker
536 the tolerance (i.e., the capacity to cope with the damage induced by the infection). As expected, we
537 found that coinfected hosts were less tolerant (i.e., steeper slope) to Py infection compared to single
538 infected mice (table 9; fig. 7f).

539

540

541

542

543

Table 9. General linear mixed model investigating the relationship between RBC counts (log 10^6/µl) and parasitemia (log proportion iRBC) in single Py infected and coinfected (Hp infecting first and simultaneous infection) mice. We report the parameter estimates with the 95% CI, degrees of freedom (df), F and p values. Mouse ID was included as a random effect to take into account the non-independence of observations for the same individual over time. N = 48 individuals and 298 observations.

Fixed effects		**Estimate**	**95% CI**	**df**	**F**	**P**
Infection				1,248	8.71	0.0035
	Single	0				
	Coinfection	-0.199	-0.331/-0.066			
Parasitemia		-0.300	-0.341/-0.259	1,248	646.17	<0.0001
Infection*Parasitemia				1,248	9.14	0.0028
	Single	0				
	Coinfection	-0.081	-0.134/-0.028			
Random effect		**Estimate**	**SE**	**z**	**p**	
Mouse ID		0.015	0.006	2.51	0.0061	

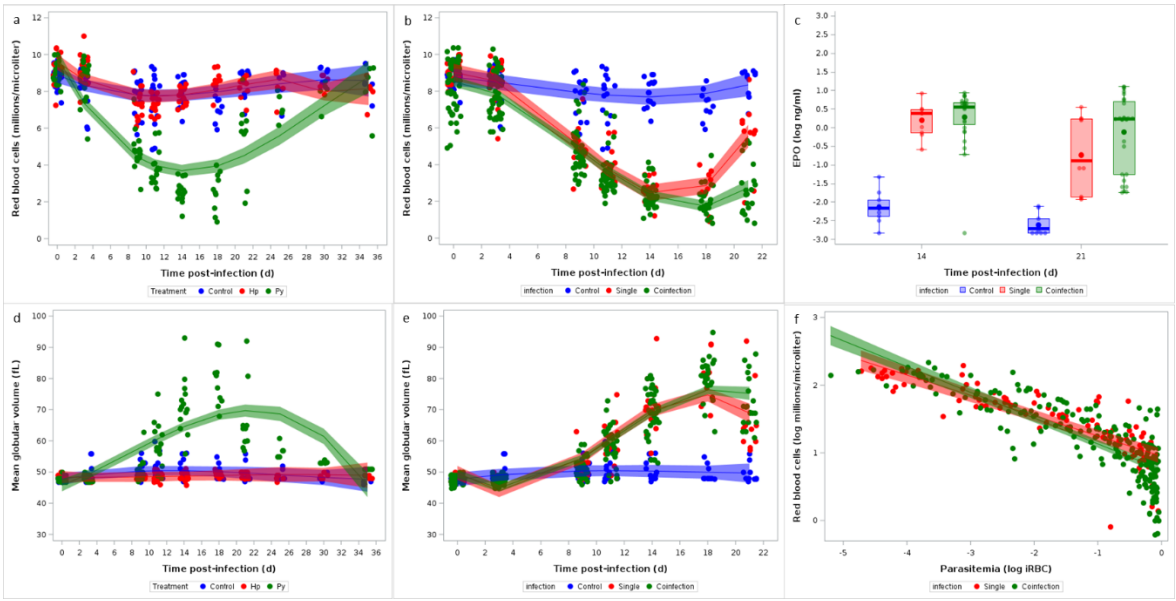

Figure 7. Effect of infection and coinfection on RBCs. a) Changes in RBC counts measured by hematology analyzer for non-infected and single (Hp, Py) infected mice; b) Changes in RBCs for non-infected, single Py infected and coinfected (Hp infecting first and simultaneous infection) groups. Dots represent the raw data, the lines represent the fit of the GLMM, and the shaded area around the line the 95% CI. c) Levels of erythropoietin (EPO, log ng/ml) in the plasma assessed by ELISA at day 14 and 21 p.i. in non-infected, single Py infected and coinfected (Hp infecting first and simultaneous infection) mice. Dots represent the raw data, the boxes represent the interquartile range (IQR), the horizontal lines the median, and whiskers the range of data within 1.5 the IQR; d) Changes in mean globular volume (MGV, fL) assessed by hematology analyzer for non-infected and single (Hp, Py) infected mice; e) Changes in MVG for non-infected, single Py infected and coinfected (Hp infecting first and simultaneous infection) groups. Dots represent the raw data, the lines represent the fit of the GLMM, and the shaded area around the line the 95% CI; f) Log-log plot of RBC counts on parasitemia for single Py infected and coinfected (Hp infecting first and simultaneous infection) groups. Dots represent the raw data, the lines represent the fit of the GLMM, and the shaded area around the line the 95% CI.

567 If coinfected hosts suffer from more severe disease symptoms because they cannot effectively
568 restore RBCs lost during the infection, we should expect that experimentally inducing erythropoiesis
569 might, at least partially, dampen the cost of coinfection. To explore this hypothesis, we ran an
570 experiment where mice were first infected with Hp and after 28 days they were infected with Py. These
571 coinfected mice were then treated with a rEPO or left as control. We assessed the severity of the
572 symptoms using an integrative marker of health (body mass), a specific marker of Py infection (changes
573 in RBCs), and any mortality (reaching of the end points) that might have occurred during the course of
574 the infection.

575 As predicted, treating coinfected mice with rEPO reduced the severity of the disease
576 symptoms, since body mass remained stable over the course of the infection, while mice in the control
577 group lost body mass from day 14 p.i. onwards (table 10, fig. 8a). rEPO treatment only slightly affected
578 anemia (GLMM, time p.i.*treatment, $F_{1,129} = 4.12$, $p = 0.0443$, n = 20 individuals and 153 observations;
579 fig. 8b, fig. S14), and although mortality was higher in the control group, the difference was not
580 statistically significant (Log-rank test, $\chi^2_1 = 1.059$, $p = 0.3034$, n = 20; fig. 8c), suggesting that other
581 aspects of the pathophysiology of coinfection might explain the observed increase in Py virulence.
582 Nevertheless, the rEPO administration improved the tolerance to Py infection, since coinfected mice
583 treated with rEPO had similar slope relating RBC counts to parasitemia as single Py infected hosts
584 (GLMM, treatment*parasitemia, $F_{1,111} = 0.11$, $p = 0.7363$, n = 25 individuals and 138 observations; fig.
585 8d). Therefore, coinfection reduced the tolerance to Py infection and administering rEPO partially
586 restored it.
587
588
589
590
591
592

Table 10. General linear mixed model investigating the changes in body mass (g) in coinfected (Hp-28+Py) mice treated or not treated with rEPO. We report the parameter estimates with the 95% CI, degrees of freedom (df), F and p values. Mouse ID was included as a random effect to take into account the non-independence of observations for the same individual over time. N = 20 individuals and 245 observations.

Fixed effects		**Estimate**	**95% CI**	**df**	**F**	**P**
Treatment				1,221	0.27	0.6055
	Control	0				
	rEPO	-0.35	-1.67/0.98			
Time		0.2	0.11/0.29	1,221	31.59	<0.0001
Squared time		-0.012	-0.016/-0.008	1,221	40.36	<0.0001
Time*Treatment				1,221	0.75	0.3878
	Control	0				
	rEPO	-0.05	-0.18/0.069			
Squared Time*Treatment				1,221	6.78	0.0098
	Control	0				
	rEPO	0.007	0.002/0.013			
Random effect		**Estimate**	**SE**	**z**	**p**	
ID		1.77	0.61	2.91	0.0018	

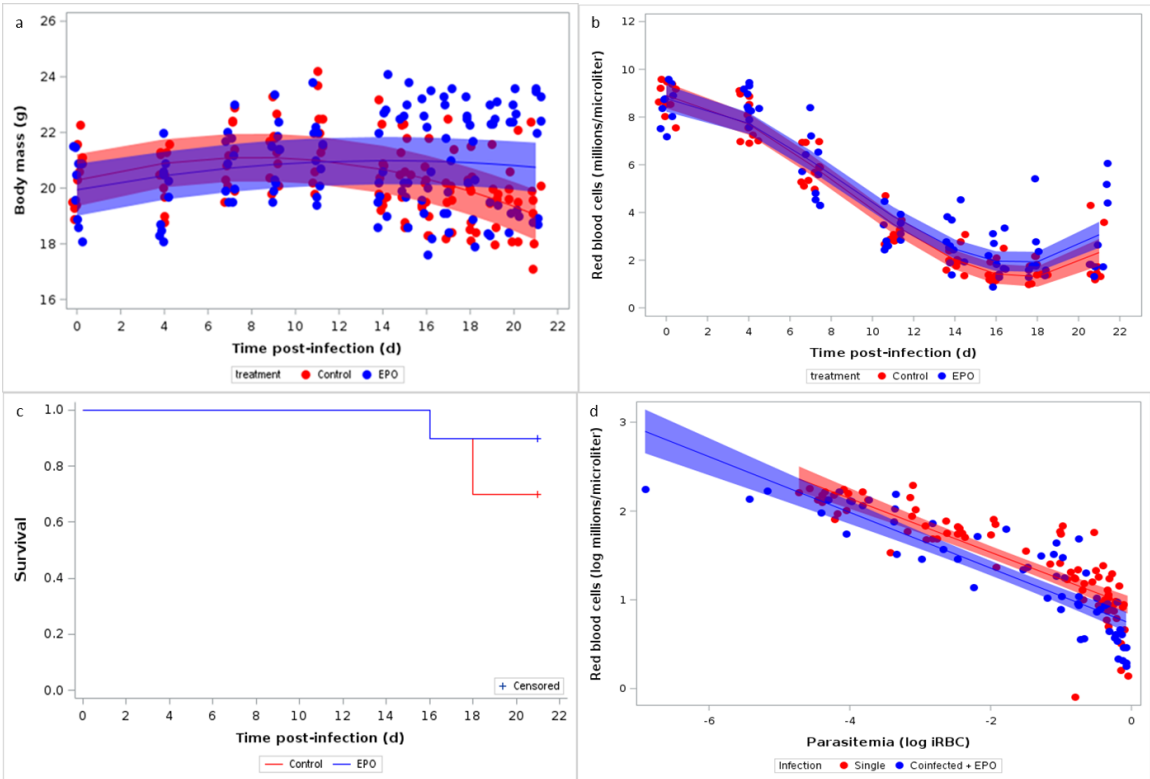

Figure 8. Effect of rEPO administration on the symptoms of the coinfection. a) Changes in body mass (g) over the course of the infection in mice that were infected with Hp at day -28 and with Py at day 0, and treated with rEPO or left as control; b) Changes in RBC counts assessed by hematology analyzer in coinfected mice treated with EPO or left as control. Dots represent the raw data, the lines represent the fit of the GLMM, and the shaded area around the line the 95% CI; c) Survival of coinfected mice treated with rEPO or left as control; d) Log-log plot of RBC counts on parasitemia for single Py infected mice and coinfected (infected with Hp at day -28 and with Py at day 0) mice treated with rEPO. Dots represent the raw data, the lines represent the fit of the GLMM, and the shaded area around the line the 95% CI.

609 In addition to inducing anemia, the lysis of RBCs releases free heme groups that have pro-
610 oxidant and pro-inflammatory properties, and stimulates the production of enzymes whose role is to
611 scavenge them. We therefore hypothesized that the increased virulence of Py in coinfected hosts
612 (when Py follows Hp) might stem from an impaired capacity to detoxify free heme groups. To this
613 purpose, we assessed the expression of the *Hmox1* gene in splenocytes at day 14 p.i. and the amount
614 of circulating heme oxygenase-1 (HO-1) in plasma at day 14 and 21 post-infection. *Hmox1* was strongly
615 upregulated in Py infected mice compared to non-infected individuals (GLM, $F_{1,8} = 96.92$, n = 10; $p <$
616 0.0001; fig. 9a, fig. S15a), and it was also upregulated in coinfected groups (groups 4, 5, 6) compared
617 to single Py infected hosts (post-hoc comparison of LS-means, $p = 0.0074$, n = 28; fig. 9a, fig. S15a,b).
618 However, although single Py infected mice also had much higher plasma levels of the enzyme HO-1 at
619 both day 14 and 21 p.i. compared to non-infected individuals (GLM, $F_{1,24} = 82.98$, $p < 0.0001$, n = 28;
620 fig. 9b), coinfected groups (groups 4, 5, 6) did not differ from single Py infection (when considering the
621 different coinfection groups separately, GLM, $F_{3,68} = 2.49$, $p = 0.0677$, n = 76; fig. S15c; when
622 considering the coinfection groups together, post-hoc comparison of LS-means, $p = 1$, n = 86; fig. 9b).
623 Therefore, although *Hmox1* gene expression was upregulated in the coinfection groups, the level of
624 the enzyme in the blood did not differ between single infection and coinfection.

625 Another important function related to the clearance of free hemoglobin is provided by the
626 scavenger receptor CD163 expressed on red pulp macrophages (RPM, F4/80$^+$ CD11b$^-$) (Kristiansen et
627 al. 2001). We therefore assessed the proportions of RPM that were CD163$^+$, by flow cytometry, and
628 compared them between non-infected and single Py infected and found that the population of CD163$^+$
629 RPM drastically dropped during the infection (generalized linear model with a beta distribution of
630 errors, $F_{1,35} = 344.88$, $p < 0.0001$, n = 39; fig. 9c). However, the proportion of RPM that were CD163$^+$
631 was similarly reduced in coinfected mice (groups 4, 5, 6) compared to single Py infection, at both day
632 14 and 21 p.i. (LS-means comparison with Bonferroni correction, day 14 p.i., $p = 0.1648$, day 21 p.i., p
633 $= 0.1959$, n = 100; fig. 9c, fig. S15d). The receptor CD163 was also less expressed in F4/80$^+$ CD11b$^-$ of
634 Py infected mice, as shown by the drastic drop in mean fluorescence intensity (MFI), with no difference

635 between single and coinfected mice (LS-means comparison with Bonferroni correction, day 14 p.i., p =
636 1, day 21 p.i., p = 1, n = 100; fig. 9d). Therefore, the population of CD163^{+} RPM which are a key resident
637 cell population responsible for clearing free hemoglobin released during the lysis of RBCs similarly
638 decreased in single and coinfected mice.

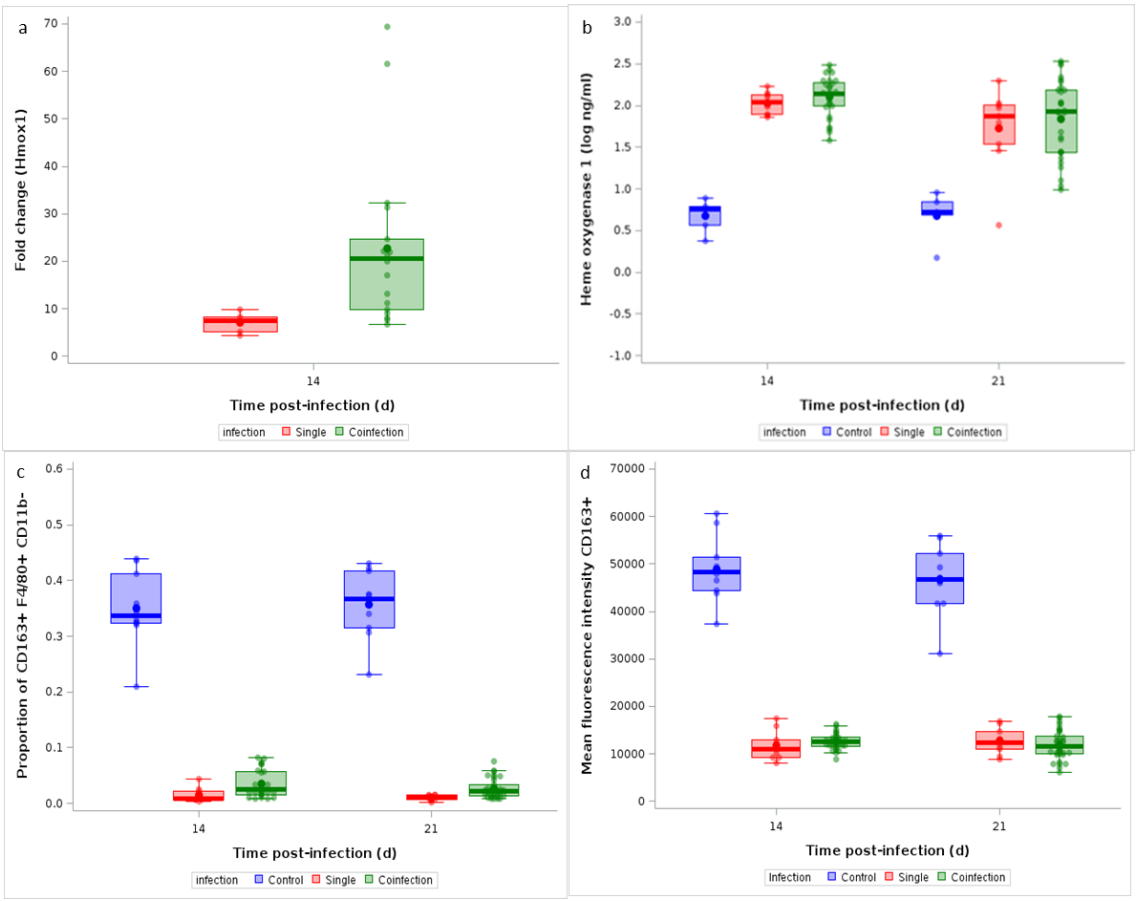

639
640 Figure 9. Effect of infection and coinfection on heme detoxification. a) Fold change of *Hmox1* mRNA in
641 spleen at day 14 p.i. in single Py infected and coinfected (Hp infecting first and simultaneous infection)
642 groups; b) Levels of Heme oxygenase-1 in the plasma (log ng/ml) at day 14 and 21 p.i. in non-infected,
643 single Py infected and coinfected (Hp infecting first and simultaneous infection) groups; c) Proportion
644 of CD163^{+} within F4/80^{+} CD11b^{-} cells analyzed by flow cytometry at day 14 and 21 p.i. in non-infected,
645 single Py infected and coinfected (Hp infecting first and simultaneous infection) groups; d) Mean
646 fluorescence intensity (arbitrary fluorescence units) of CD163 at day 14 and 21 p.i. in non-infected,
647 single Py infected and coinfected (Hp infecting first and simultaneous infection) groups. Dots represent
648 the raw data, the boxes represent the interquartile range (IQR), the horizontal lines the median, and
649 whiskers the range of data within 1.5 the IQR.
650
651 ***Immune predictors of Py virulence***
652
653 *Plasmodium* infection elicits proinflammatory effectors that might cause immunopathology if
654 regulatory mechanisms fail to restore homeostasis. Therefore, we speculated that exacerbated disease
655 severity in coinfected hosts (when Py follows Hp) might stem from an overreacting, non-regulated,

656 inflammatory response. To address this question, we first assessed the gene expression of pro- and
657 anti-inflammatory cytokines in splenocytes at day 3 and 14 post-infection. IFN-γ, IL-10 and TGF-β1
658 genes were all overexpressed at both 3 and 14 days p.i. in single Py infected hosts compared to non-
659 infected mice (GLM, IFN-γ, $F_{1,34} = 24.44$, $p < 0.001$; IL-10, $F_{1,34} = 49.86$, $p < 0.001$; TGF-β, $F_{1,34} = 20.62$, p
660 < 0.001, n = 38; fig. 10; fig. S16a,b,c). However, coinfection (groups 4, 5, 6) did not induce a change in
661 the expression of any of the genes compared to single Py infection (LS-means comparison with
662 Bonferroni correction, all p's = 1, fig. 10, fig. S16d,e,f).

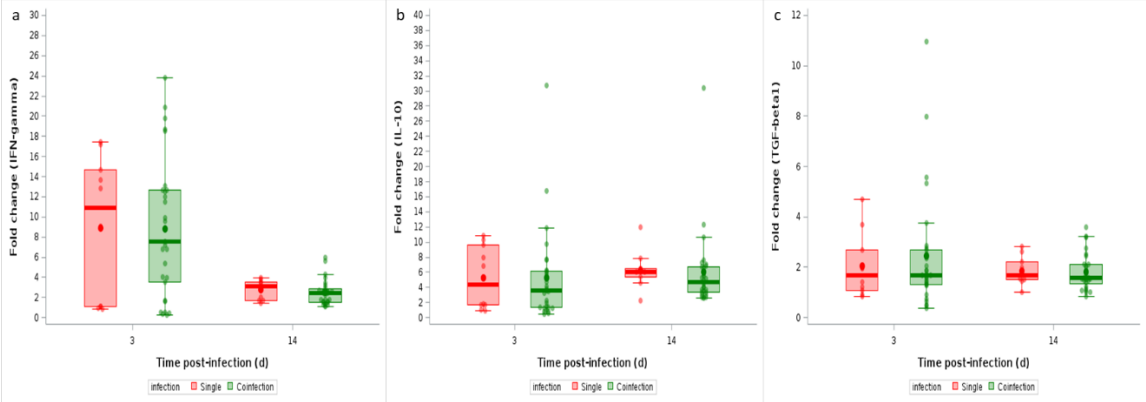

663
664 Figure 10. Effect of infection and coinfection on cytokine expression. Fold change of a) IFN-γ, b) IL-10,
665 c) TGF-β1 mRNA levels in spleen at day 3 and 14 p.i. in single Py infected and coinfected (Hp infecting
666 first and simultaneous infection) groups. Dots represent the raw data, the boxes represent the
667 interquartile range (IQR), the horizontal lines the median, and whiskers the range of data within 1.5
668 the IQR.
669
670 Previous work conducted on the same model system has shown that coinfected mice have a
671 higher activation of regulatory T cells (Treg), possibly accounting for their impaired anti-*Plasmodium*
672 response (Tetsutani et al. 2009). Therefore, we assessed the proportions of $CD4^+$ T cells that were
673 $FoxP3^+$ by flow cytometry and compared them, over the course of the infection, between non-infected,
674 single Py infected and coinfected mice (groups 4, 5, 6); we found no differences between single Py
675 infection and coinfection groups (LS-means comparison with Bonferroni correction, p = 1; n = 100; fig.
676 11a, table S15; fig. S17a). The expression of the immune check point CTLA-4 on Treg has been shown
677 to impede immunity to the acute infection with Py (Kurup et al. 2017), by enhancing their
678 immunosuppressive activity. We thus assessed the proportions of $CD4^+$ T cells that were $FoxP3^+$ and
679 $CTLA\text{-}4^+$ by flow cytometry and compared them between non-infected, single Py infected and

680 coinfected mice (groups 4, 5, 6); we found that coinfected mice had a higher proportion of CTLA-4$^+$
681 Treg compared to non-infected and single Py infection at day 14 p.i. (table 11; fig. 11b; table S16; fig.
682 S17b). Therefore, although coinfection did not produce an expansion of the Treg population compared
683 to single Py infected hosts, the immunosuppressive power of Treg was upregulated in coinfected hosts.
684

685 Table 11. Generalized linear model with a beta distribution of errors investigating the changes in the
686 proportion of CTLA-4$^+$ within FoxP3$^+$ CD4$^+$ T cells in non-infected, single Py infected and coinfected (Hp
687 infecting first and simultaneous infection) mice at day 14 and 21 post-infection. We report the degrees
688 of freedom (df), and the F and p values. N = 96 individuals.

Source of variation	df	F	P
Infection	2,90	19.01	<0.0001
Time	1,90	0.79	0.3755
Time*Infection	2,90	13.89	<0.0001

689

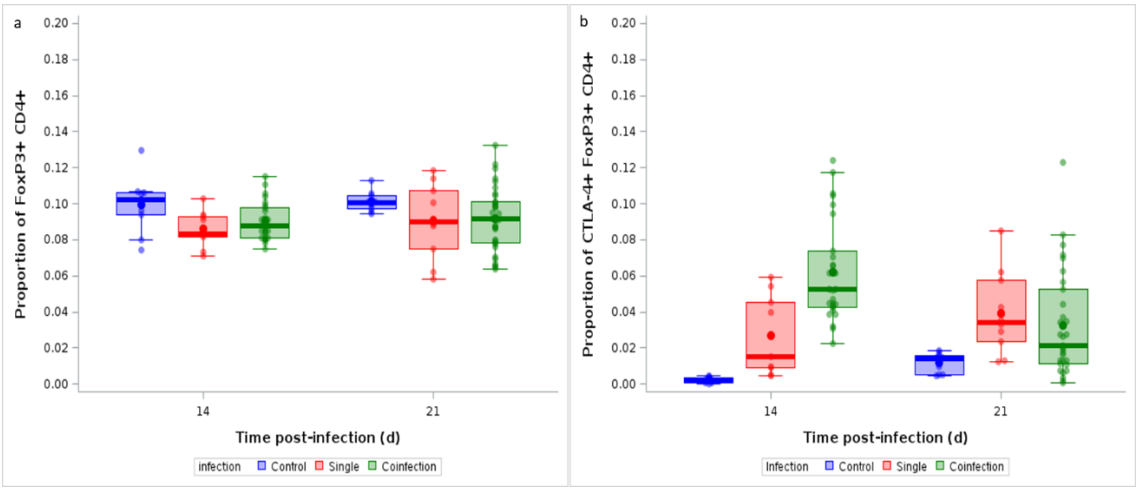

690
691 Figure 11. Effect of infection and coinfection on Treg expansion and immunosuppressive function. a)
692 Proportion of FoxP3$^+$ within CD4$^+$ T cells analyzed by flow cytometry over the course of the infection
693 in non-infected, single Py infected and coinfected (Hp infecting first and simultaneous infection) mice;
694 b) Proportion of CTLA-4$^+$ within FoxP3$^+$ CD4$^+$ T cells analyzed by flow cytometry over the course of the
695 infection in non-infected, single Py infected and coinfected (Hp infecting first and simultaneous
696 infection) mice. Dots represent the raw data, the boxes represent the interquartile range (IQR), the
697 horizontal lines the median, and whiskers the range of data within 1.5 the IQR.
698

699 Using flow cytometry, we also immunophenotyped mice using a large panel of markers in the
700 spleen (table S2), at day 3, 14 and 21 post-infection. We identified 20 cell populations (table S17) and
701 their proportions were included as variables in a principal component analysis (PCA), with a PCA per
702 sampling day. The first two components explained 29.02% and 18.79%, 39.65% and 12.86%, 37.63%
703 and 15.92% of the total variance, at day 3, 14, and 21 p.i., respectively. The correlation circles showed

704 that many of the variables included in the PCA had high absolute loadings (table S17, fig. 12a, b, c), and
705 effectively discriminated the three experimental groups (non-infected, single Py infected and
706 coinfected mice) over the course of the infection (fig. 12d,e,f).

707 At day 3 p.i., the scores along the first principal component (PC1) strongly differed between
708 the three experimental groups (GLM, $F_{2,45} = 28.56$, n = 48; $p < 0.0001$), with coinfected mice (groups 4,
709 5, 6) having higher scores compared to both non-infected and single Py infection (LS-means
710 comparisons with Bonferroni correction, both p's < 0.0001; fig. 12g). At day 14 and 21 p.i., there was
711 a complete separation, along the PC1, between the three groups, with single Py infected lying in
712 between non-infected and coinfected individuals (groups 4, 5, 6) (day 14 p.i.: GLM, $F_{2,43} = 313.37$, p <
713 0.0001, n = 46; day 21 p.i.: GLM, $F_{2,51} = 257.50$, $p < 0.0001$, n = 54; fig. 12g). The PC2 had a much less
714 discriminant power among groups (day 3 p.i.: GLM, $F_{2,45} = 3.02$, p = 0.0588, n = 48; day 14 p.i.: GLM,
715 $F_{2,43} = 1.27$, p = 0.2902, n = 46; day 21 p.i.: GLM, $F_{2,51} = 7.57$, p = 0.0013, n = 54; fig. 12h).

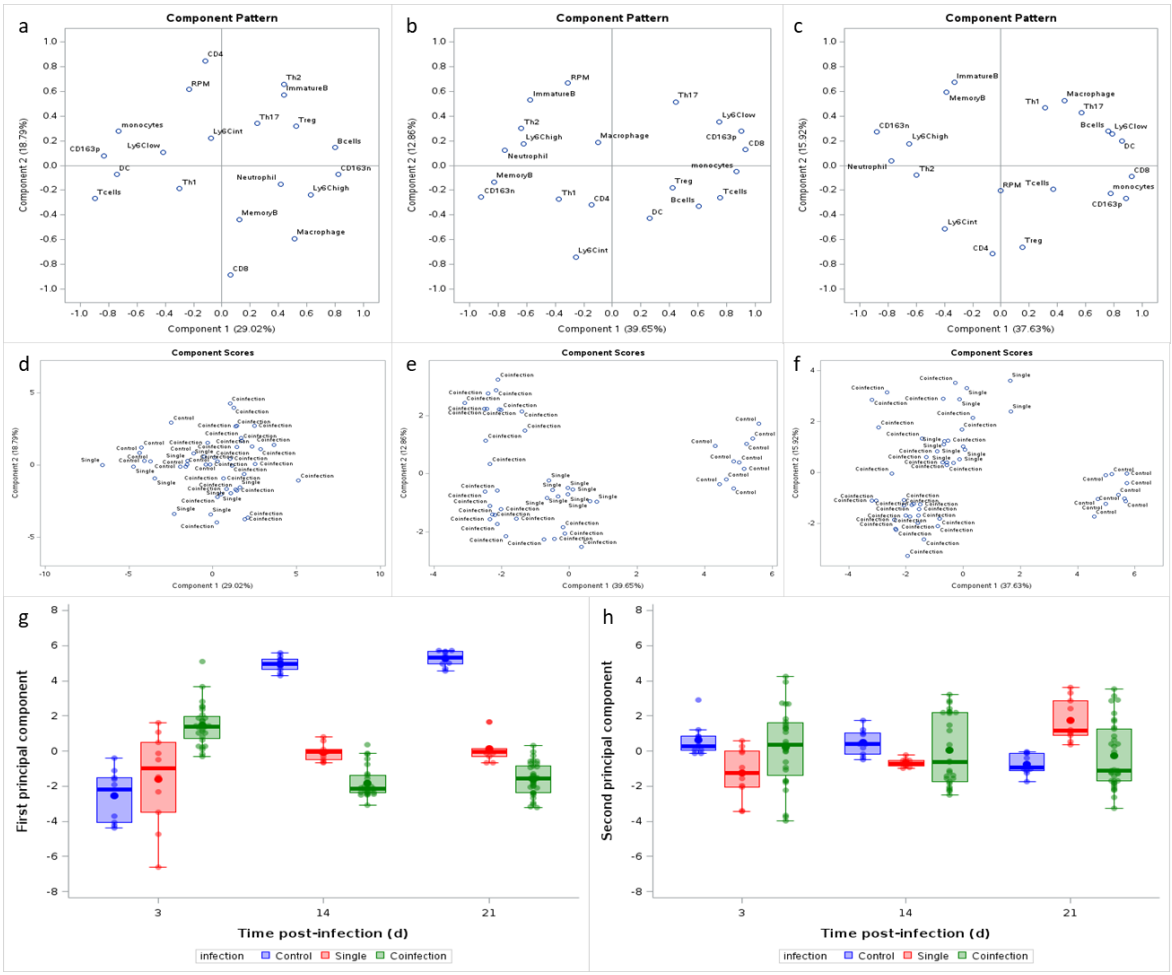

716

717 Figure 12. Immunophenotyping of spleen over the course of the infection. Principal component
718 analysis (PCA) on the proportion of 20 immune cell populations at day 3 (a,d), 14 (b,e), 21 (c,f) p.i. in
719 non-infected, single Py infected, and coinfected (Hp infecting first and simultaneous infection) hosts.
720 We report the loadings of the 20 variables on the first two components of the PCA at each sampling
721 day (a,b,c); the position of each individual host in the bivariate space defined by the PC1 and PC2,
722 according to their experimental group (d,e,f); the scores on the PC1 (g) and PC2 (h) for the three
723 experimental groups. For g) and h), dots represent the raw data, the boxes represent the interquartile
724 range (IQR), the horizontal line the median, and whiskers the range of data within 1.5 the IQR.
725

726 To go further, we focused on the variables that had strong absolute loadings on the PC1 and
727 compared them between the groups, with the aim to see if there was a consistent difference between
728 single Py infected and coinfected hosts (groups 4, 5, 6). The proportion of Th2 (proportion of $CD4^+$ T
729 cells that were GATA-3^+) differed between single and coinfected hosts at the three sampling dates
730 (GLM with a beta distribution of errors, $F_{2,139} = 53.91$, $p < 0.0001$, $n = 148$; LS-means comparison
731 between single and coinfected with Bonferroni correction, day 3, $p = 0.0002$; day 14, $p = 0.0102$; day
732 21, $p < 0.0001$; fig. 13a). Among the other variables, only $CD8^+$ T cells consistently discriminated
733 between single Py and coinfected hosts (groups 4, 5, 6), with the proportion of $CD8^+$ T cells (proportion
734 of $CD3^+$ that were $CD8^+$) sharply decreasing over time and especially so in coinfected hosts (GLM with
735 a beta distribution of errors, $F_{2,139} = 347.41$, $p < 0.0001$, $n = 148$; LS-means comparison between single
736 and coinfected with Bonferroni correction, day 3, $p = 1$; day 14, $p < 0.0001$; day 21, $p < 0.0001$, fig.
737 13b).

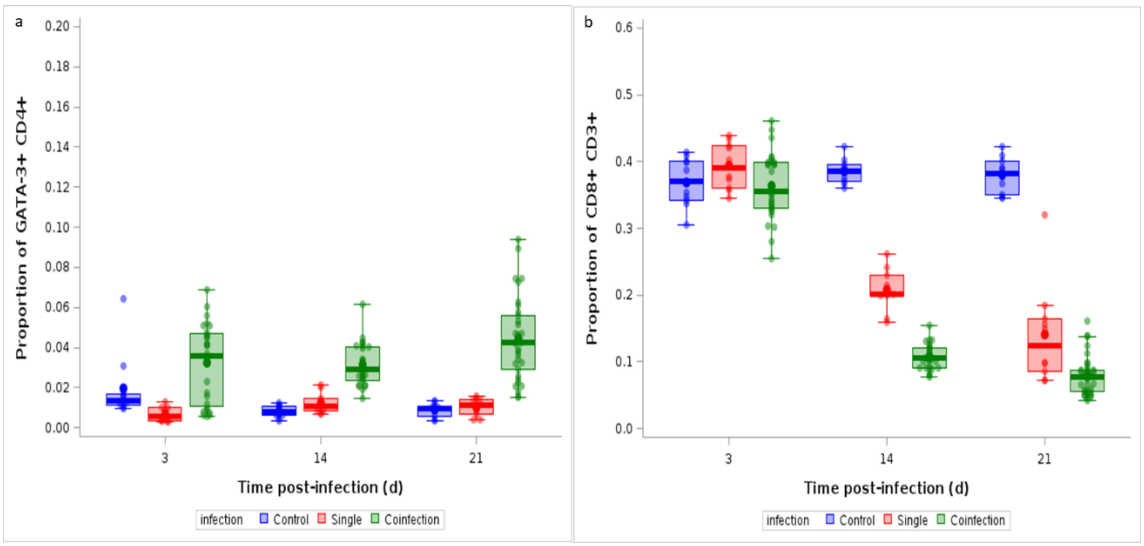

738
739 Figure 13. Effect of infection and coinfection on Th2 and $CD8^+$ T cells. a) Proportion of GATA-3^+ within
740 $CD4^+$ T cells and b) proportion of $CD8^+$ within $CD3^+$ T cells analyzed by flow cytometry over the course
741 of the infection in non-infected, single Py infected and coinfected (Hp infecting first and simultaneous

742 infection) hosts. Dots represent the raw data, the boxes represent the interquartile range (IQR), the
743 horizontal lines the median, and whiskers the range of data within 1.5 the IQR.
744

745 Therefore, Th2 and CD8$^+$ T cells were the two cell populations that best discriminated between
746 Py infected and coinfected hosts (when Py follows Hp). While the effect of coinfection on the rise of
747 Th2 lymphocytes can easily be understood as the direct consequence of Hp induction of Th2 immunity,
748 we wished to better investigate the reasons underlying the decrease of CD8$^+$ T cells in coinfected mice.
749 To this purpose, we assessed the proportion of CD8$^+$ T cells that expressed three immune checkpoints
750 in non-infected, single Py infected and coinfected hosts (groups 4, 5 and 6), and predicted that
751 coinfected mice should have higher proportions of CD8$^+$ T cells expressing the immune checkpoints
752 compared to single infection. Infection enhanced the proportion of CTLA-4$^+$ CD8$^+$ T cells (proportion of
753 CD8$^+$ that were CTLA-4$^+$) but there was no difference between single infection and coinfection at any
754 of the sampling day (GLM with a beta distribution of errors: day 14 p.i, t = -0.52, df = 90, p = 1; day 21
755 p.i., t = -1.19, df = 90, p = 1; fig. 14a). The proportions of LAG-3$^+$ CD8$^+$ and PD-1$^+$ CD8$^+$ cells (proportion
756 of CD8$^+$ that were LAG-3$^+$ and PD-1$^+$, respectively) were also increased in infected mice compared to
757 non-infected individuals, however, at day 14 p.i. there was also a higher proportion of LAG-3$^+$ and PD-
758 1$^+$ CD8$^+$ T cells in coinfected mice compared to single infection (GLM with a beta distribution of errors:
759 LAG-3, day 14 p.i.: t = 3.38, df = 91, p = 0.0163; day 21 p.i., t = 2.36, df = 91, p = 0.3040; PD-1, day 14
760 p.i.: t = 3.94, df = 90, p = 0.0024; day 21 p.i., t = 2.26, df = 91, p = 0.3948, fig. 14b,c).

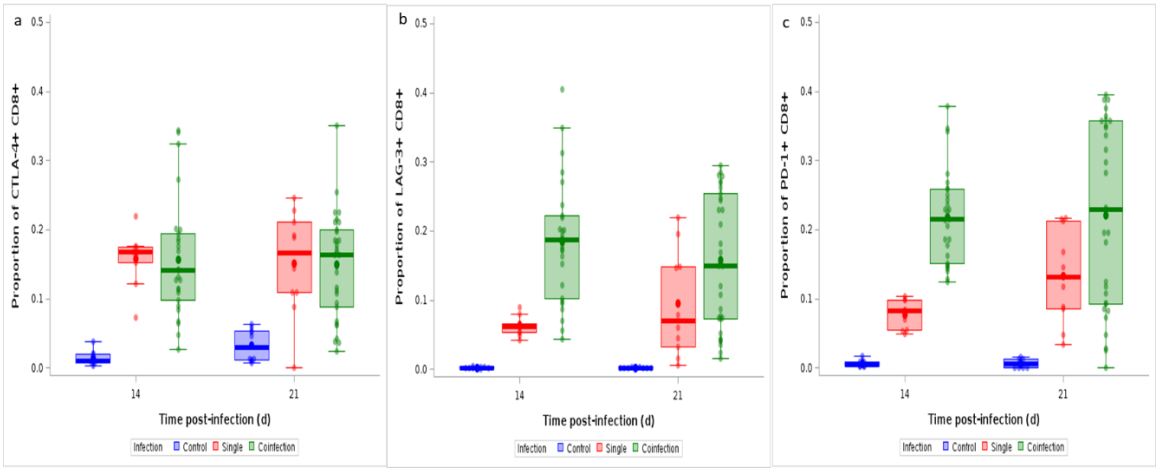

761
762 Figure 14. Effect of infection and coinfection on CD8$^+$ T cell exhaustion. a) Proportion of CTLA-4$^+$ within
763 CD8$^+$ T cells, b) LAG-3$^+$ within CD8$^+$ T cells, c) PD-1$^+$ within CD8$^+$ T cells analyzed by flow cytometry at
764 day 14 and 21 p.i. in non-infected, single Py infected and coinfected (Hp infecting first and

765 simultaneous infection) hosts. Dots represent the raw data, the boxes represent the interquartile
766 range (IQR), the horizontal lines the median, and whiskers the range of data within 1.5 the IQR.
767

768 Persistent antigenic stimulation and high levels of inhibitory receptors (immune checkpoints)
769 can lead to the exhaustion of $CD8^+$ T cells, characterized by a loss of effector functions and proliferative
770 potential (McLane et al. 2019), that could explain the increase in the $CD4^+/CD8^+$ ratio above the
771 homeostatic value (between 1.5 and 2.5) (McBride and Striker 2017). Deviations from this homeostatic
772 value have been associated with severe symptoms in a few infectious diseases (e.g., Pascual-Dapena
773 et al. 2022). We therefore wished to investigate if high values of the $CD4^+/CD8^+$ ratio also predicted
774 mortality in our system. We could not investigate this point at the individual level because data on the
775 proportion of immune cells were gathered on mice that were euthanized at specific days post-
776 infection. Nevertheless, we could correlate the $CD4^+/CD8^+$ ratio at day 14 and 21 p.i. with the mortality
777 rate (the proportion of mice reaching the end points) within each experimental group and found that
778 indeed the higher the ratio the higher the mortality risk (spearman correlation, Rs = 0.766, n = 100, p
779 < 0.0001, fig. 15).

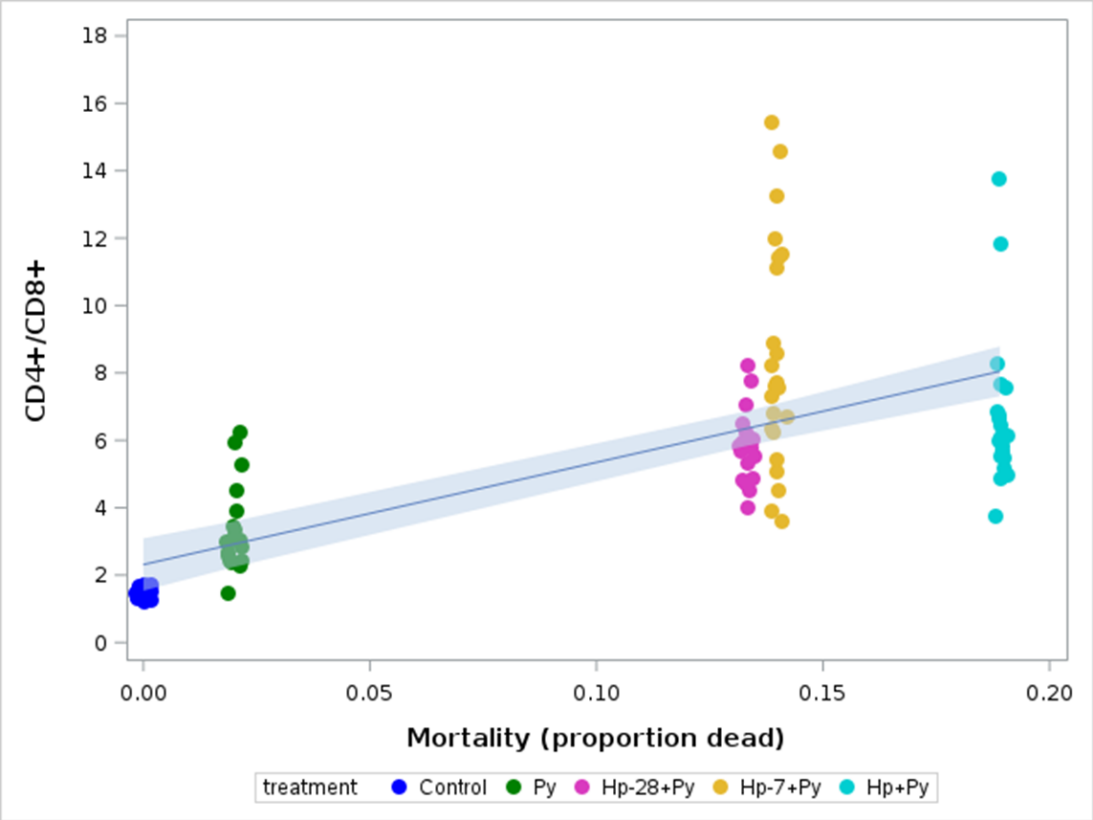

780

781 Figure 15. Correlation between the $CD4^+/CD8^+$ ratio at day 14 and 21 p.i. and the mortality rate in non-
782 infected, single Py infected and coinfected (Hp infecting first and simultaneous infection) hosts.
783 Mortality refers to the proportion of hosts reaching the experimental end points within groups. Dots
784 represent the raw data, the line a linear regression fit and the band the 95% CI of the slope.
785
786 **Discussion**
787
788 We showed that the order of infection plays a paramount role in determining the outcome of
789 the coinfection between an intestinal nematode and a *Plasmodium* parasite. In particular, Py virulence
790 substantially increased when infecting hosts that were previously (or simultaneously) infected with Hp,
791 compared both to hosts with single infections and to hosts that were infected with Py first and then
792 with Hp. Contrary to Py, virulence of Hp was minimally affected by the coinfection, since Hp only
793 produced mild symptoms whatever the order of the infection. These results are partially in agreement
794 with our initial predictions. We hypothesized that previous infection with either Py or Hp would
795 polarize the immune response towards Th1 or Th2 effectors making the ground more favorable for a
796 subsequent infection, and resulting in more severe disease symptoms. This prediction was met when
797 Py infected mice harboring Hp, but not when Hp infected mice harboring Py. Therefore, there is a
798 strong asymmetry in the effect of coinfection between Py and Hp, depending on the order of the
799 infection. The increase in Py virulence in mice previously infected with Hp is consistent with previous
800 results on this system (Tetsutani et al. 2009), suggesting that previous Hp infection impairs the
801 subsequent immune response to Py (Noland et al. 2008; Tetsutani et al. 2009).
802 The possible evolutionary reasons underlying this asymmetry are manifold. Intestinal
803 nematodes usually produce chronic infections where the hosts keep shedding parasite eggs for months
804 or even years depending on the species (Morand 1996). Inter-host transmission success and parasite
805 fitness is tightly associated with the duration of egg shedding (patent period), therefore any parasite
806 trait that compromises host health and survival is likely counter selected in these systems. In
807 agreement with this view, nematode infections are usually well tolerated and host damage is usually
808 observed only when parasite burden is high (Brooker 2010; Lippens et al. 2016). Since reinfection was
809 not possible in our experiment, parasite burden was constrained by the initial number of infective
810 larvae given to the host. It might be interesting to investigate to what extent the lack of increase in Hp

811 virulence in coinfected hosts could change when using higher infective doses (Lippens et al. 2016), or
812 allowing hosts to be reinfected. Although the transmission success of Py cannot be directly assessed
813 from the proportion of iRBC, longer persistence of high parasite density, as observed in coinfected
814 hosts, should increase the likelihood of gametocyte production, as reported for other *Plasmodium*
815 species (see Tadesse et al. 2017). In agreement with this view, Py transmission success to the dipteran
816 vector was enhanced when mice were coinfected with the helminth *Echinostoma caproni* (Noland et
817 al. 2007). Therefore, the cost of virulence is probably higher in Hp than in Py. Alternatively, increased
818 Py virulence might be maladaptive if host overexploitation and death jeopardize parasite fitness
819 through reduced transmission success.

820 Whatever the benefit or disadvantage of changes in virulence for Py, from the host
821 perspective, coinfection did incur costs both in terms of general health and specific markers of Py
822 infection. In particular, whether single infected hosts still gained mass during the 5 weeks p.i., at a rate
823 that was similar to the non-infected hosts, coinfection induced a loss of body mass (when Py infected
824 mice previously infected with Hp) or temporarily slowed down the gain in body mass (when Hp infected
825 mice previously infected with Py). In agreement with the results on changes in body mass, host
826 mortality (reaching of the end points) was only reported in coinfection groups where Py followed the
827 Hp infection. Interestingly, there was no difference according to the timing of the infection, suggesting
828 that the importance of the order of the infection is conserved and relatively consistent over different
829 coinfection scenarios. In another coinfection model, involving the cestode *Taenia crassiceps* and
830 *Plasmodium yoelii* 17XL, Salazar-Castañón et al. (2018) found that coinfected mice had relatively longer
831 survival time compared to single Py infected hosts and that the gain in survival was related to the
832 timing of the infection (the longer the delay between the infection, the better the gain in survival time),
833 suggesting that the effect of timing of infection might be model-dependent.

834 Our prediction of increased virulence in coinfected hosts was based on the rationale that
835 previous infection with nematodes polarizes the immune system towards a Th2 response (Reynolds et
836 al. 2012). In agreement with this hypothesis, we found that Th2 indeed discriminated the three

837 experimental groups, with higher percentage of GATA-3^{+} within CD4^{+} T cells in coinfected hosts (when
838 Py follows Hp) compared to both single Py infected and non-infected mice. Accordingly, we also
839 predicted that coinfected mice should have an impaired capacity to deal with the Py infection and
840 indeed we found that parasitemia was still high at day 21 p.i. in coinfected hosts compared to single
841 Py infected mice. Therefore, direct damage produced by Py multiplication might account for the more
842 severe disease symptoms observed in coinfected hosts. In agreement with this view, changes in RBC
843 counts over the course of the infection mirrored changes in parasitemia, with coinfected groups still
844 suffering from anemia at day 21 p.i., when single Py infected mice had already started to recover.

845 The fitness consequences of the damage caused by Py multiplication also depend on the host
846 capacity to repair damaged tissues, or in other terms on the capacity to tolerate the infection
847 (Medzhitov et al. 2012). In particular, RBCs are constantly renewed during hematopoiesis and
848 therefore hosts that can restore lost RBCs at a faster pace should be able to better tolerate the
849 infection (i.e., to pay a smaller infection cost) compared to hosts with a slower rate of RBC renewal
850 (Chang et al. 2004). Given that coinfected hosts suffered from higher anemia, compensating for the
851 higher rate of RBC loss would have needed a higher production of reticulocytes. However, we found
852 that coinfected hosts had similar plasma levels of EPO and similar proportions of reticulocytes, as
853 assessed by the MGV, compared to single infected hosts. Therefore, despite higher parasitemia and
854 higher anemia, coinfected hosts only replaced RBCs at a similar rate of single infected hosts, and
855 therefore were less tolerant to the Py infection. This finding suggests that any improvement of the
856 capacity to renew lost RBCs should reduce the cost of coinfection. Indeed, experimental administration
857 of rEPO to coinfected hosts partially improved the symptoms of the disease, as also previously reported
858 (Kaiser et al. 2006), and improved host tolerance to the infection. However, the magnitude of the
859 effects was small, suggesting that other aspects of the physiopathology of the coinfection are probably
860 more important determinants of the coinfection costs. In addition, the production of reticulocytes also
861 replenishes the reservoir of cells that can be exploited by Py for its own replication, which can also

862 contribute to maintain parasitemia over longer period of time and possibly exacerbates disease
863 severity (Chang et al. 2004; Tsubata et al. 2005).

864 Massive release of free heme groups has the potential to damage host tissues through their
865 prooxidant, proinflammatory and cytotoxic effects (Kumar and Bandyopadhyay 2005; Immenschuh et
866 al. 2017). Previous studies have shown that the effectiveness of the mechanisms of detoxification of
867 free heme groups are key determinants of host survival (Pamplona et al. 2007; Seixas et al. 2009) and
868 liver function restoring once the parasite has been cleared (Dey et al. 2014), although the anti-
869 inflammatory properties of HO-1 might also promote liver infection (Epiphanio et al. 2008). We
870 therefore assessed the expression of the *Hmox1* gene in splenocytes and the amount of the enzyme
871 HO-1 in plasma. As for the renewal of lost RBCs, given that coinfected hosts had higher amount of free
872 hemoglobin compared to single infection (due to the higher RBC lysis), we expected to find a higher
873 expression of *Hmox1* and more HO-1 in plasma of coinfected hosts. However, although the gene was
874 overexpressed in coinfected mice (the gene was highly overexpressed in infected mice compared to
875 non-infected hosts), the amount of enzyme was similar in coinfected and single Py infected hosts,
876 possibly due to the degradation of the enzyme through the ubiquitin-proteasome system (Lin et al.
877 2008; Chau 2015). We also found that another mechanism allowing the host to deal with free
878 hemoglobin (the scavenger receptor CD163) (Kristiansen et al. 2001) was downregulated in RPM of
879 coinfected and single infected hosts.

880 Free heme group is also recognized as a DAMP by the immune system and can induce an
881 overreacting inflammatory response leading to host damage (Fortes et al. 2012). Coinfection between
882 Hp and another model species of murine malaria (*Plasmodium chabaudi* AS) has been reported to
883 increase host mortality (Su et al. 2005), due to liver pathology involving hepatic IFN-γ, IL-17 and IL-22
884 (Helmby 2009). Although infected hosts overexpressed IFN-γ, IL-10 and TGF-β1 compared to non-
885 infected mice, there was no difference between coinfected and single Py infected mice. Similarly, we
886 did not find any difference in the percentage of $FoxP3^+$ within $CD4^+$ T cells between single Py infected
887 and coinfected mice; however, the percentage of CTLA-4^+ within $FoxP3^+$ $CD4^+$ T cells was higher in

888 coinfected mice compared to single Py infected hosts during the peak of the acute infection. Therefore,
889 although we did not find an expansion of Treg in Py infected mice (as previously shown, Tetsutani et
890 al. 2009), the immunosuppressive capacities of Treg were upregulated in single Py infected mice, and
891 even more so in coinfected hosts through the CTLA-4 immune checkpoint (see Kurup et al. 2017).
892 Therefore, coinfected mice appeared to have an upregulated immunosuppressive function, possibly
893 accounting for the failure to control Py multiplication.

894 We went a step further by identifying 20 immune cell populations in the spleen by spectral
895 flow cytometry using a 27-color panel. The results of the PCA clearly showed that the three
896 experimental groups clustered in different areas of the space defined by the first two components,
897 and especially so at day 14 and 21 p.i., with the single Py infection group lying in between the non-
898 infected and the coinfection groups. The cell population that best discriminated between single Py
899 infected and coinfected hosts was the $CD8^+$ T cells that got exhausted more in coinfected mice. Several
900 Py epitopes are recognized by $CD8^+$ T cells during the blood stage of the infection (Howland et al. 2015).
901 Moreover, previous work has shown that $CD8^+$ T cells play a role in the protective immunity against
902 blood-stage infection with Py (Imai et al. 2010), and chronic infection with the nematode *Litosomoides*
903 *sigmodontis* interferes with the anti-*Plasmodium* $CD8^+$ T cell response (Kolbaum et al. 2012). Infection
904 with Hp has also been shown to suppress $CD8^+$ T cells in mice subsequently infected with the protozoan
905 *Toxoplasma gondii* (Khan et al. 2008). Exhaustion of $CD8^+$ cells results from the overexpression of
906 immune checkpoints whose function is to avoid immunopathology during persistent antigenic
907 exposure (Chandele et al. 2010; Wykes and Lewin 2018; McLane et al. 2019). In agreement with this,
908 we found that the proportion of both PD-1^+ and LAG-3^+ within $CD8^+$ T cells was higher in coinfected
909 hosts compared to single Py infection at day 14 post-infection. Mechanisms supposed to protect the
910 hosts from immunopathology (Howland et al. 2015) might thus actually make them more susceptible
911 to parasite exploitation (Scholzen et al. 2009; Frimpong et al. 2019), and especially so when hosts are
912 coinfected by parasites with different exploitation strategies.

913 One of the consequences of the $CD8^+$ exhaustion is an increase of the ratio between $CD4^+$ and
914 $CD8^+$ T cells. Deviations of the $CD4^+/CD8^+$ ratio from the homeostatic values (inverted ratio below 1, or
915 increased values above 2.5) have been investigated in a few host-pathogen systems, and found to
916 correlate with poor host survival prospects (McBride and Striker 2017). For instance, high values of the
917 $CD4^+/CD8^+$ ratio have been shown to be predictors of patient mortality during SARS-CoV-2 infection
918 (De Zunai et al. 2021; Pascual-Dapena et al. 2022). We found similar results, although the correlation
919 between the $CD4^+/CD8^+$ ratio and mortality could only be assessed at the population (inter-group)
920 level. The increase of the $CD4^+/CD8^+$ ratio probably reflects a global, temporary, dysfunction of the
921 immune response, which favors the replication rate of Py in coinfected hosts. In agreement with this
922 view, BALB/c mice infected with Py and depleted of $CD8^+$ T cells suffered from greater parasitemia and
923 higher mortality compared to control individuals during the period of peak parasitemia (Imai et al.
924 2015).

925 This work provides some relevant findings for the epidemiology of the coinfection between
926 nematodes and *Plasmodium* and possibly for the evolution of virulence when parasites exploit the
927 same host. In terms of the epidemiology of the disease, a key question is whether infection order is
928 random or if it intrinsically depends on the life cycle of the parasite. We suggest that, in the specific
929 case of the coinfection between gastrointestinal nematodes and *Plasmodium*, hosts might have higher
930 chances to suffer from ordered infections where *Plasmodium* infects hosts already harboring worms.
931 This suggestion is based on the observation that gastrointestinal nematodes usually establish chronic,
932 steady state, infections that can last for months (or even years for some human helminths) while
933 *Plasmodium* produces acute infections (lasting 2-4 weeks) that can either be cleared or lead to
934 subsequent relapses (again depending on the parasite and the host species). However, this hypothesis
935 rests on the assumption that hosts have equal probabilities to be infected by the two parasites per unit
936 of time, or in other words that the probability of infection is not age-dependent. It should also be
937 reminded that our experimental work only considered primary infections (reinfection was not
938 allowed). However, in the real world, hosts are repeatedly exposed to multiple parasites and when

939 there is no sterilizing immunity, previous infection does not fully prevent subsequent reinfection. The
940 complexity due to age-dependent probability of infection and repeated exposure/infection might
941 therefore blur the importance of the infection order as a driver of disease severity.

942 We also think that these results are relevant to predict how selection might shape the optimal
943 level of virulence (defined as infection-induced host damage) when parasites exploit hosts that harbor
944 coinfecting parasites that elicit different immune effectors. A key prediction here is that species-
945 specific cost of virulence might constraint the evolution of host damage in different ways in coinfecting
946 parasites. Experimental evolution and theoretical modelling would be valuable tools to explore this
947 question.

948 A final thought is that, although we considered that the coinfection dynamics with *Plasmodium*
949 and nematodes is regulated by top-down mechanisms involving the host immune response, we cannot
950 ignore that both parasites (and nematodes in particular) can also interfere with the host immune
951 response for their own benefit. This paves the way for a scenario where the top-down mechanisms
952 might also be under parasite control.

953

954 **Acknowledgments**

955 We are grateful to Valérie Saint Giorgio and all the staff of the animal facility for taking care of the
956 animals.

957 **Funding**

958 The work has been funded by the French Agence Nationale de la Recherche (grant # ANR-21-CE35-
959 0015).

960 **Author contribution**

961 GS, BF, MR and BR conceived the study and gathered the funding; AD, LB, NP, GS and BF collected the
962 data; AD, LB, EG performed the lab work; NP assisted with the spectral flow cytometry analysis; GS
963 analyzed the data; GS, AD and LB wrote the first draft of the manuscript; all authors revised and
964 approved the final version.

965 **Data availability statement**

966 All the data will be made available in DRYAD once the manuscript has been accepted for publication.

967 **Conflict of interest**

968 The authors declare no conflict of interest.

969

970 **References**

971 Adegnika AA, Kremsner PG. 2012. Epidemiology of malaria and helminth interaction: e review from
972 2001 to 2011. Current Opinion in HIV and AIDS 7: 221-224.

973 Afolabi MO, Ale BM, Dabira ED, Agbla SC, Bustinduy AL, Ndiaye JLA, Greenwood B. 2021. Malaria and
974 helminth co-infections in children living in endemic countries: A systematic review with meta-
975 analysis. PLoS Neglected Tropical Diseases 15: e0009138.

976 Alizon S, de Roode JC, Michalakis Y. 2013. Multiple infections and the evolution of virulence. Ecology
977 Letters 16, 556-567.

978 Bansemir AD, Sukhdeo MVK. 1994. The food resource of adult *Heligmosomoides polygyrus* in the small
979 intestine. Journal of Parasitology 80, 24.

980 Billet LS, Wuerthner VP, Hua J, Relyea RA, Hoverman JT. 2020. Timing and order of exposure to two
981 echinostome species affect patterns of infection in larval amphibians. Parasitology 147: 1515-
982 1523.

983 Brooker S. 2010. Estimating the global distribution and disease burden of intestinal nematode
984 infections: Adding up the numbers – A review. International Journal for Parasitology 40: 1137-
985 1144.

986 Budischak SA, Wiria AE, Hamid F, Wammes LJ, Kaisar MMM, van Lieshout L, Sartono E, Supali T,
987 Yazdanbakhsh M, Graham AL. 2018. Competing for blood: the ecology of parasite resource
988 competition in human malaria-helminth co-infections. Ecology Letters 21: 536.

989 Chandele A, Mukerjee P, Das G, Ahmed R, Chauhan VS. Phenotypic and functional profiling of malaria-
990 induced CD8 and CD4 T cells during blood-stage infection with *Plasmodium yoelii*. Immunology
991 132: 273-286.
992 Chang K-H, Tam M, Stevenson MM. 2004. Modulation of the course and outcome of blood-stage
993 malaria by erythropoietin-induced reticulocytosis. The Journal of Infectious Diseases 189: 735-
994 743.
995 Chau L-Y. 2015. Heme oxygenase-1: emerging target of cancer therapy. Journal of Clinical Science 22:
996 22.
997 Clay PA, Rudolf VHW. 2019. How parasite interaction strategies alter virulence evolution in multi-
998 parasite communities. Evolution 73: 2189.
999 Coelho CH, Gazzinelli-Guimaraes PH, Howard J, Barnafo E, Alani NAH, Muratova O, McCormack A,
1000 Kelnhofer E, Urban Jr JF, Narum DL, Anderson C, Langhorne J, Nutman TB, Duffy PE. 2019.
1001 Chronic helminth infection does not impair immune response to malaria transmission blocking
1002 vaccine Pfs230D1-EPA/Alhydrogel® in mice. Vaccine 37: 1038-1045.
1003 Craig JM, Scott AL. 2017. Antecedent *Nippostrongylus* infection alters the lung immune response to
1004 *Plasmodium berghei*. Parasite Immunology 39: e12441.
1005 Degarege A, Erko B. 2016. Epidemiology of *Plasmodium* and helminth coinfection and possible reasons
1006 for heterogeneity. BioMed Research International 2016: 3083568.
1007 Degarege A, Veledar E, Degarege D, Erko B, Nacher M, Madhivanan P. 2016. *Plasmodium falciparum*
1008 and soil-transmitted helminth co-infections among children in sub-Saharan Africa: a systematic
1009 review and meta-analysis. Parasite Vectors 9: 344.
1010 Dey S, Mazumder S, Siddiqui AA, Iqbal MS, Banerjee C, Sarkar S, De R, Goyal M, Bindu S,
1011 Bandyopadhyay U. 2014. Association of heme oxygenase 1 with the restoration of liver function
1012 after damage in murine malaria by *Plasmodium yoelii*. Infection and Immunity 8: 3113-3126.

1013 De Zuani M, Laznickova P, Tomaskova V, Dvoncovan M, Forte G, Stokin GB, Sramek V, Helan M, Fric J.
1014 2022. High CD4-to-CD8 ratio identifies an at-risk population susceptible to lethal COVID-19.
1015 Scandinavian Journal of Immunology 95: e13125.
1016 Epiphanio S, Mikolajczak SA, Gonçalves LA, Pamplona A, Portugal S, Albuquerque S, Goldberg M,
1017 Rebelo S, Anderson DG, Akinc A, Vomlocher H-P, Kappe SHI, Soares MP, Mota MM. Heme
1018 oxygenase-1 is an anti-inflammatory host factor that promotes murine *Plasmodium* liver
1019 infection. Cell Host & Microbe 3: 331-338.
1020 Ezenwa VO, Jolles AE. 2011. From host immunity to pathogen invasion: the effects of helminth
1021 coinfection on the dynamics of microparasites. Integrative and Comparative Biology 51: 540.
1022 Fenton A. 2013. Dances with worms: the ecological and evolutionary impacts of deworming on
1023 coinfecting pathogens. Parasitology 140: 1119-1132.
1024 Filbey KJ, Camberis M, Chandler J, Turner R, Kettle AJ, Eichenberger RM, Giacomin P, Le Gros G. 2019.
1025 Intestinal helminth infection promotes IL-5- and $CD4^+$ T cell-dependent immunity in the lung
1026 against migrating parasites. Mucosal Immunology 12: 352-362.
1027 Fortes GB, Alves LS, de Oliveira R, Dutra FF, Rodrigues D, Fernandez PL, Souto-Padron, T, De Rosa MJ,
1028 Kelliher M, Golenbock D, Chan FKM, Bozza MT. 2012. Heme induces programmed necrosis on
1029 macrophages through autocrine TNF and ROS production. Blood 119: 2368-2375.
1030 Frimpong A, Kusi KA, Adu-Gyasi D, Amponsah J, Ofori MF, Ndifon W. 2019. Phenotypic evidence of T
1031 cell exhaustion and senescence during symptomatic *Plasmodium falciparum* malaria. Frontiers
1032 in Immunology 10: 1345.
1033 Graham AL. 2008. Ecological rules governing helminth-microparasite coinfection. PNAS 105: 566.
1034 Gregory RD Montgomery SSJ, Montgomery WI. 1992. Population biology of *Heligmosomoides*
1035 *polygyrus* (Nematoda) in the wood mouse. Journal of Animal Ecology 61: 749-757.
1036 Griffiths EC, Fairlie-Clarke K, Allen JE, Metcalf CJE, Graham AL. 2015. Bottom-up regulation of malaria
1037 population dynamics in mice co-infected with lung-migratory nematodes. Ecology Letters 18:
1038 1387-1396.

1039 Hartgers FC, Yazdanbakhsh M. 2006. Co-infection of helminths and malaria: modulation of the immune
1040 responses to malaria. Parasite Immunology 28: 497.
1041 Helmby H. 2009. Gastrointestinal nematode infection exacerbates malaria-induced liver pathology.
1042 Journal of Immunology 182: 5663.
1043 Howland SW, Claser C, Poh CM, Gun SY, Rénia L. 2015. Pathogenic $CD8^+$ T cells in experimental cerebral
1044 malaria. Seminars in Immunopathology 37: 221-231.
1045 Hürlimann E, Houngbedji CA, Yapi RB, N'Dri PB, Silué KD, Ouattara M, Utzinger J, N'Goran EK, Raso G.
1046 2019. Antagonistic effects of *Plasmodium*-helminth co-infection on malaria pathology in
1047 different population groups in Côte d'Ivoire. PLoS Neglected Tropical Diseases 13: e0007086.
1048 Imai T, Shen J, Chou B, Duan X, Tu L, Tetsutani K, Moriya C, Ishida H, Hamano S, Shimokawa C, Hisaeda
1049 H, Himeno K. 2010. Involvement of $CD8^+$ T cells in protective immunity against murine blood-
1050 stage infection with *Plasmodium yoelii* 17XL strain. European Journal of Immunology 40: 1053-
1051 1061.
1052 Imai T, Ishida H, Suzue K, Taniguchi T, Okada H, Shimokawa C, Hisaeda H. 2015. Cytotoxic activities of
1053 $CD8^+$ T cells collaborate with macrophages to protect against blood-stage murine malaria. eLIFE
1054 4: e04232.
1055 Imrie R, Walsh SK, Roberts KE, Lello J, Longdon B. 2023. Investigating the outcomes of virus coinfection
1056 within and across host species. PLoS Pathogens 19: e1011044.
1057 Immenschuh S, Vijayan V, Janciauskiene S, Gueler F. 2017. Heme as a target for therapeutic
1058 interventions. Frontiers in Pharmacology 8: 146.
1059 Kaiser K, Texier A, Ferrandiz J, Meiller A, Latour C, Peyron F, Cespuglio R, Picot S. 2006. Recombinant
1060 human erythropoietin prevents the death of mice during cerebral malaria. Journal of Infectious
1061 Diseases 193: 987-995.
1062 Karvonen A, Jokela J, Laine A-L. 2019. Importance of sequence and timing in parasite coinfections.
1063 Trends in Parasitology 35: 109-118.

1064 Khan IA, Hakak R, Eberle K, Sayles P, Weiss LM, Urban Jr JF. 2008. Coinfection with *Heligmosomoides*
1065 *polygyrus* fails to establish CD8$^+$ T-cell immunity against *Toxoplasma gondii*. Infection and
1066 Immunity 76: 1305-1313.
1067 Knowles SCL. 2011. The effect of helminth co-infection on malaria in mice: a meta-analysis.
1068 International Journal for Parasitology 41: 1041.
1069 Kolbaum J, Escbach M-L, Steeg C, Jacobs T, Fleischer B, Breloer M. 2012. Efficient control of
1070 *Plasmodium yoelii* infection in BALB/c and C57BL/6 mice with pre-existing *Strongyloides ratti*
1071 infection. Parasite Immunology 34: 388-393.
1072 Kolbaum J, Tartz S, Hartmann W, Helm S, Nagel A, Heussler V, Sebo P, Fleischer B, Jacobs T, Breloer M.
1073 2012. Nematode-induced interference with the anti-Plasmodium CD8$^+$ T-cell response can be
1074 overcome by optimizing antigen administration. European Journal of Immunology 42: 890-900.
1075 Kotepui M, Mala W, Kwankaew P, Kotepui KU, Ramirez Masangkay F, Wilairatana P. 2023. Distinct
1076 cytokine profiles in malaria coinfection: A systematic review. PLoS Neglected Tropical Diseases
1077 17: e0011061.
1078 Kristiansen M, Graversen JH, Jacobsen C, Sonne O, Hoffman HJ, Law SK, Moestrup SK. 2001.
1079 Identification of the haemoglobin scavenger receptor. Nature 409: 198-201.
1080 Kumar S, Bandyopadhyay U. 2005. Free heme toxicity and its detoxification systems in human.
1081 Toxicology Letters 157: 175-188.
1082 Kurup SP, Obeng-Adjei N, Anthony SM, Traore B, Doumbo OK, Butler NS, Crompton PD, Harty JT. 2017.
1083 Regulatory T cells impede acute and long-term immunity to blood-stage malaria through CTLA-
1084 4. Nature Medicine 23: 1220-1227.
1085 Kwan JL, Seitz AE, Fried M, Lee K-L, Metenou S, Morrison R, Kabyemela E, Nutman TB, Prevots DR,
1086 Duffy PE. 2018. Seroepidemiology of helminths and the associations with severe malaria among
1087 infants and young children in Tanzania. PLoS Neglected Tropical Diseases 12: e0006345.

1088 Lin P-H, Chiang M-T, Chau L-Y. 2008. Ubiquitin-proteasome system mediates heme oxygenase-1
1089 degradation through endoplasmatic reticulum-associated degradation pathway. Biochimica et
1090 Biophysica Acta 1783: 1826-1834.
1091 Lippens C, Guivier E, Faivre B, Sorci G. 2016. Reaction norms of host immunity, host fitness and parasite
1092 performance in a mouse - intestinal nematode interaction. International Journal for Parasitology
1093 46: 133-140.
1094 Ma Y, Su X-Z, Lu F. 2020. The roles of Type I interferon in co-infections with parasites and viruses,
1095 bacteria, or other parasites. Frontiers in Immunology 11: 1805.
1096 McBride JA, Striker R. 2017. Imbalance in the game of T cells: What can the CD4/CD8 T-cell ratio tell us
1097 about HIV and health? PLoS Pathogens 13: e1006624.
1098 McLane, L, Abdel-Hakeem MS, Wherry EJ. 2019. CD8 T cell exhaustion during chronic viral infection
1099 and cancer. Annual Review of Immunology 37: 457-495.
1100 Medzhitov R, Schneider DS, Soares MP. 2012. Disease tolerance as a defense strategy. Science 335:
1101 936-941.
1102 Morand S. 1996. Life-history traits in parasitic nematodes: a comparative approach for the search of
1103 invariants. Functional Ecology 10: 210-218.
1104 Nacher M. 2011. Interactions between worms and malaria: good worms or bad worms? Malaria
1105 Journal 10: 259.
1106 Noland GS, Chowdhury DR, Urban Jr JF, Zavala F, Kumar N. 2010. Helminth infection impairs the
1107 immunogenicity of a *Plasmodium falciparum* DNA vaccine, but not irradiated sporozoites, in
1108 mice. Vaccine 28: 2917-2923.
1109 Noland GS, Graczyk TK, Fried B, Kumar N. 2007. Enhanced malaria parasite transmission from helminth
1110 co-infected mice. American Journal of Tropical Medicine and hygiene 76: 1052.
1111 Noland GS, Urban JF, Fried B, Kumar N. 2008. Counter-regulatory anti-parasite cytokine responses
1112 during concurrent *Plasmodium yoelii* and intestinal helminth infections in mice. Experimental
1113 Parasitology 119: 272-278.

1114 Olatunde AC, Cornwall DH, Roedel M, Lamb TJ. 2022. Mouse models for unravelling immunology of
1115 blood stage malaria. Vaccines 10: 1525.
1116 Paludan SR. 1998. Interleukin-4 and interferon-γ: the quintessence of a mutual antagonistic
1117 relationship. Scandinavian Journal of Immunology 48: 459-468.
1118 Pamplona A, Ferreira A, Balla J, Jeney V, Balla G, Epiphanio S, Chora A, Rodrigues CD, Gregoire IP,
1119 Cunha-Rodrigues M, Portugal S, Soares MP, Mota MM. 2007. Heme oxygenase-1 and carbon
1120 monoxide suppress the pathogenesis of experimental cerebral malaria. Nature Medicine 13:
1121 703–710.
1122 Pascual-Dapena A, Chillaron JJ, Llauradó G, Arnau-Barres I, Flores J, Lopez-Montesinos I, Sorlí L,
1123 Martinez-Pérez JL, Gómez-Zorrilla S, Du J, García-Giralt N, Güerri-Fernández R. 2022. Individuals
1124 with higher CD4/CD8 ratio exhibit increased risk of acute respiratory distress syndrome and in-
1125 hospital mortality during acute SARS-CoV-2 infection. Frontiers in Medicine 9: 924267.
1126 Reynolds LA, Filbey KJ, Maizels RM. 2012. Immunity to the model intestinal helminth parasite
1127 *Heligmosomoides polygyrus*. Seminars in Immunopathology 34: 829-846.
1128 Salazar-Castañón VH, Juárez-Avelar I, Legorreta-Herrera M, Govezensky T, Rodriguez-Sosa M. 2018.
1129 Co-infection: the outcome of *Plasmodium* infection differs according to the time of pre-existing
1130 helminth infection. Parasitology Research 117: 2767.
1131 Salazar-Castañón VH, Legorreta-Herrera M, Rodriguez-Sosa M. 2014. Helminth parasites alter
1132 protection against *Plasmodium* infection. BioMed Research International 2014: 913696.
1133 Scholzen A, Minigo G, Plebanski M. 2009. Heroes or villains? T regulatory cells in malaria infection.
1134 Trends in Parasitology 26: 16-25.
1135 Seixas E, Gozzelino R, Chora A, Ferreira A, Silva G, Larsen R, Rebelo S, Penido C, Smith NR, Coutinho A,
1136 Soares MP. 2009. Heme oxygenase-1 affords protection against noncerebral forms of severe
1137 malaria. Proceedings of the National Academy of Sciences 106: 15837-15842.

1138 Segura M, Matte C, Thawani N, Su Z, Stevenson MM. 2009. Modulation of malaria-induced
1139 immunopathology by concurrent gastrointestinal nematode infection in mice. International
1140 Journal for Parasitology 39: 1525.
1141 Shen S-S, Qu X-Y, Zhang W-Z, Li J, Lv Z-Y. 2019. Infection against infection: parasite antagonism against
1142 parasites, viruses and bacteria. Infectious Diseases of Poverty 8: 49.
1143 Su Z, Segura M, Morgan K, Loredo-Osti JC, Stevenson MM. 2005. Impairment of protective immunity
1144 to blood-stage malaria by concurrent nematode infection. Infection and Immunity 73: 3531-
1145 3539.
1146 Su Z, Segura M, Stevenson MM. 2006. Reduced protective efficacy of a blood-stage malaria vaccine by
1147 concurrent nematode infection. Infection and Immunity 74: 2138-2144.
1148 Supali T, Verweij JJ, Wiria AE, Djuardi Y, Hamid F, Kaisar MMM, Wammes LJ, van Lieshout L, Luty AJF,
1149 Sartoro E, Yazdanbakhsh M. 2010. Polyparasitism and its impact on the immune system.
1150 International Journal for Parasitology 40: 1171-1176.
1151 Szabo E, Bowhay C, Forrester E, Liu H, Dong B, Coria AL, Perera S, Fung B, Badawadagi N, Gaio C, Bailey
1152 K, Ritz M, Bowron J, Ariyaratne A, Finney CAM. 2024. *Heligmosomoides bakeri* and *Toxoplasma*
1153 *gondii* co-infection leads to increased mortality associated with changes in immune resistance
1154 in the lymphoid compartment and disease pathology. PLoS ONE 19: e02922408.
1155 Tadesse FG, van den Hoogen L, Lanke K, Schildkraut J, Tetteh K, Aseffa A, Mamo H, Sauerwein R, Felger
1156 I, Drakeley C, Gadissa E, Bousema T. 2017. The shape of the iceberg: quantification of
1157 submicroscopic *Plasmodium falciparum* and *Plasmodium vivax* parasitemia and gametocytemia
1158 in five low endemic settings in Ethiopia. Malaria Journal 16: 99.
1159 Tetsutani K, Ishiwata K, Ishida H, Tu L, Torii M, Hamano S, Himeno K, Hisaeda H. 2009. Concurrent
1160 infection with *Heligmosomoides polygyrus* suppresses anti-*Plasmodium yoelii* protection
1161 partially by induction of $CD4^{+}CD25^{+}Foxp3^{+}$ Treg in mice. European Journal of Immunology 39:
1162 2822-2830.

1163 Tsubata S, Ebe K, Kawamura T, Ishimoto Y, Tomiyama-Miyaji C, Watanabe H, Sekikawa H, Aoyagi Y,
1164 Abo T. 2005. Protection against malaria by anti-erythropoietin antibody due to suppression of
1165 erythropoiesis in the liver and at other sites. Immunology and Cell Biology 83: 638-642.
1166 Viney ME, Graham AL. 2013. Patterns and processes in parasite co-infection. Advances in Parasitology
1167 82: 321-369.
1168 Wait LF, Kamiya T, Fairlie-Clarke KJ, Metcalf CJE, Graham AL, Mideo N. 2021. Differential drivers of
1169 intraspecific and interspecific competition during malaria-helminth co-infection. Parasitology
1170 148: 1030-1039.
1171 Webb EL, Ekii AO, Pala P. 2012. Epidemiology and immunology of helminth-HIV interactions. Current
1172 Opinion in HIV and AIDS 7: 245-253.
1173 Wykes MN, Lewin SR. 2018. Immune checkpoint blockade in infectious diseases. Nature Reviews
1174 Immunology 18: 91-104.